

World Journal of *Stem Cells*

World J Stem Cells 2024 June 26; 16(6): 615-738



EDITORIAL

- 615 Searching for the optimal precondition procedure for mesenchymal stem/stromal cell treatment: Facts and perspectives
Zhao YD, Huang YC, Li WS
- 619 Gut microbiota modulating intestinal stem cell differentiation
He L, Zhu C, Zhou XF, Zeng SE, Zhang L, Li K
- 623 Priming mesenchymal stem cells to develop “super stem cells”
Haider KH

ORIGINAL ARTICLE**Clinical Trials Study**

- 641 Safety and efficiency of Wharton’s Jelly-derived mesenchymal stem cell administration in patients with traumatic brain injury: First results of a phase I study
Kabatas S, Civelek E, Boyalı O, Sezen GB, Ozdemir O, Bahar-Ozdemir Y, Kaplan N, Savrunlu EC, Karaöz E

Basic Study

- 656 RPLP0/TBP are the most stable reference genes for human dental pulp stem cells under osteogenic differentiation
Ferreira DB, Gasparoni LM, Bronzeri CF, Paiva KBS
- 670 Mesenchymal stem cells-extracellular vesicles alleviate pulmonary fibrosis by regulating immunomodulators
Gao Y, Liu MF, Li Y, Liu X, Cao YJ, Long QF, Yu J, Li JY
- 690 Outcomes of combined mitochondria and mesenchymal stem cells-derived exosome therapy in rat acute respiratory distress syndrome and sepsis
Lin KC, Fang WF, Yeh JN, Chiang JY, Chiang HJ, Shao PL, Sung PH, Yip HK
- 708 Exosomes from umbilical cord mesenchymal stromal cells promote the collagen production of fibroblasts from pelvic organ prolapse
Xu LM, Yu XX, Zhang N, Chen YS
- 728 Umbilical cord mesenchymal stem cell exosomes alleviate necrotizing enterocolitis in neonatal mice by regulating intestinal epithelial cells autophagy
Zhu L, He L, Duan W, Yang B, Li N

ABOUT COVER

Editorial Board Member of *World Journal of Stem Cells*, Tong Ming Liu, PhD, Senior Research Scientist, Cell Biology and Therapies, Institute of Molecular and Cell Biology, Singapore 138673, Singapore. dbsliutm@yahoo.com

AIMS AND SCOPE

The primary aim of *World Journal of Stem Cells (WJSC, World J Stem Cells)* is to provide scholars and readers from various fields of stem cells with a platform to publish high-quality basic and clinical research articles and communicate their research findings online. *WJSC* publishes articles reporting research results obtained in the field of stem cell biology and regenerative medicine, related to the wide range of stem cells including embryonic stem cells, germline stem cells, tissue-specific stem cells, adult stem cells, mesenchymal stromal cells, induced pluripotent stem cells, embryonal carcinoma stem cells, hemangioblasts, lymphoid progenitor cells, *etc.*

INDEXING/ABSTRACTING

The *WJSC* is now abstracted and indexed in Science Citation Index Expanded (SCIE, also known as SciSearch®), Journal Citation Reports/Science Edition, PubMed, PubMed Central, Scopus, Biological Abstracts, BIOSIS Previews, Reference Citation Analysis, China Science and Technology Journal Database, and Superstar Journals Database. The 2024 Edition of Journal Citation Reports® cites the 2023 journal impact factor (JIF) for *WJSC* as 3.6; JIF without journal self cites: 3.5; 5-year JIF: 4.2; JIF Rank: 16/31 in cell and tissue engineering; JIF Quartile: Q3; and 5-year JIF Quartile: Q3; JIF Rank: 105/205 in cell biology; JIF Quartile: Q3; and 5-year JIF Quartile: Q2. The *WJSC*'s CiteScore for 2023 is 7.8 and Scopus CiteScore rank 2023: Histology is 11/62; Genetics is 78/347; Genetics (clinical) is 19/99; Molecular Biology is 131/410; Cell Biology is 104/285.

RESPONSIBLE EDITORS FOR THIS ISSUE

Production Editor: *Xiang-Di Zhang*; Production Department Director: *Xu Guo*; Cover Editor: *Jia-Ru Fan*.

NAME OF JOURNAL

World Journal of Stem Cells

ISSN

ISSN 1948-0210 (online)

LAUNCH DATE

December 31, 2009

FREQUENCY

Monthly

EDITORS-IN-CHIEF

Shengwen Calvin Li, Carlo Ventura

EDITORIAL BOARD MEMBERS

<https://www.wjgnet.com/1948-0210/editorialboard.htm>

PUBLICATION DATE

June 26, 2024

COPYRIGHT

© 2024 Baishideng Publishing Group Inc

INSTRUCTIONS TO AUTHORS

<https://www.wjgnet.com/bpg/gerinfo/204>

GUIDELINES FOR ETHICS DOCUMENTS

<https://www.wjgnet.com/bpg/GerInfo/287>

GUIDELINES FOR NON-NATIVE SPEAKERS OF ENGLISH

<https://www.wjgnet.com/bpg/gerinfo/240>

PUBLICATION ETHICS

<https://www.wjgnet.com/bpg/GerInfo/288>

PUBLICATION MISCONDUCT

<https://www.wjgnet.com/bpg/gerinfo/208>

ARTICLE PROCESSING CHARGE

<https://www.wjgnet.com/bpg/gerinfo/242>

STEPS FOR SUBMITTING MANUSCRIPTS

<https://www.wjgnet.com/bpg/GerInfo/239>

ONLINE SUBMISSION

<https://www.f6publishing.com>

Basic Study

Outcomes of combined mitochondria and mesenchymal stem cells-derived exosome therapy in rat acute respiratory distress syndrome and sepsis

Kun-Chen Lin, Wen-Feng Fang, Jui-Ning Yeh, John Y Chiang, Hsin-Ju Chiang, Pei-Lin Shao, Pei-Hsun Sung, Hon-Kan Yip

Specialty type: Cell and tissue engineering

Provenance and peer review: Unsolicited article; Externally peer reviewed.

Peer-review model: Single blind

Peer-review report's classification

Scientific Quality: Grade A, Grade C

Novelty: Grade B

Creativity or Innovation: Grade B

Scientific Significance: Grade B

P-Reviewer: Susak YM, Ukraine

Received: January 18, 2024

Revised: April 8, 2024

Accepted: May 9, 2024

Published online: June 26, 2024

Processing time: 159 Days and 7.4 Hours



Kun-Chen Lin, Department of Anesthesiology, Kaohsiung Chang Gung Memorial Hospital, Kaohsiung 83301, Taiwan

Wen-Feng Fang, Division of Pulmonary and Critical Care Medicine, Department of Internal Medicine, Kaohsiung Chang Gung Memorial Hospital, Chang Gung University College of Medicine, Kaohsiung 83301, Taiwan

Jui-Ning Yeh, Department of Cardiology, The First Affiliated Hospital of Jinan University, Guangzhou 510630, Guangdong Province, China

John Y Chiang, Department of Computer Science and Engineering, National Sun Yat-sen University, Kaohsiung 804201, Taiwan

John Y Chiang, Department of Healthcare Administration and Medical Informatics, Kaohsiung Medical University, Kaohsiung 80708, Taiwan

Hsin-Ju Chiang, School of Medicine, Chung Shan Medical University, Taichung 40201, Taiwan

Pei-Lin Shao, Hon-Kan Yip, Department of Nursing, Asia University, Taichung 41354, Taiwan

Pei-Hsun Sung, Hon-Kan Yip, Division of Cardiology, Department of Internal Medicine, Kaohsiung Chang Gung Memorial Hospital and Chang Gung University College of Medicine, Kaohsiung 83301, Taiwan

Pei-Hsun Sung, Hon-Kan Yip, Institute for Translational Research in Biomedicine, Kaohsiung Chang Gung Memorial Hospital, Kaohsiung 83301, Taiwan

Pei-Hsun Sung, Hon-Kan Yip, Center for Shockwave Medicine and Tissue Engineering, Kaohsiung Chang Gung Memorial Hospital, Kaohsiung 83301, Taiwan

Hon-Kan Yip, Department of Medical Research, China Medical University Hospital, China Medical University, Taichung 40402, Taiwan

Hon-Kan Yip, School of Medicine, College of Medicine, Chang Gung University, Taoyuan 33302, Taiwan

Co-corresponding authors: Pei-Hsun Sung and Hon-Kan Yip.

Corresponding author: Hon-Kan Yip, MD, Chief Doctor, Division of Cardiology, Department of Internal Medicine, Kaohsiung Chang Gung Memorial Hospital and Chang Gung University College of Medicine, No. 123 Dapi Road, Niasung District, Kaohsiung 83301, Taiwan. han.gung@msa.hinet.net

Abstract

BACKGROUND

The treatment of acute respiratory distress syndrome (ARDS) complicated by sepsis syndrome (SS) remains challenging.

AIM

To investigate whether combined adipose-derived mesenchymal-stem-cells (ADMSCs)-derived exosome (EX^{AD}) and exogenous mitochondria (mito^{Ex}) protect the lung from ARDS complicated by SS.

METHODS

In vitro study, including L2 cells treated with lipopolysaccharide (LPS) and *in vivo* study including male-adult-SD rats categorized into groups 1 (sham-operated-control), 2 (ARDS-SS), 3 (ARDS-SS + EX^{AD}), 4 (ARDS-SS + mito^{Ex}), and 5 (ARDS-SS + EX^{AD} + mito^{Ex}), were included in the present study.

RESULTS

In vitro study showed an abundance of mito^{Ex} found in recipient-L2 cells, resulting in significantly higher mitochondrial-cytochrome-C, adenosine triphosphate and relative mitochondrial DNA levels ($P < 0.001$). The protein levels of inflammation [interleukin (IL)-1 β /tumor necrosis factor (TNF)- α /nuclear factor- κ B/toll-like receptor (TLR)-4/matrix-metalloproteinase (MMP)-9/oxidative-stress (NOX-1/NOX-2)/apoptosis (cleaved-caspase3/cleaved-poly (ADP-ribose) polymerase)] were significantly attenuated in lipopolysaccharide (LPS)-treated L2 cells with EX^{AD} treatment than without EX^{AD} treatment, whereas the protein expressions of cellular junctions [occluding/ β -catenin/zonula occludens (ZO)-1/E-cadherin] exhibited an opposite pattern of inflammation (all $P < 0.001$). Animals were euthanized by 72 h post-48 h-ARDS induction, and lung tissues were harvested. By 72 h, flow cytometric analysis of bronchoalveolar lavage fluid demonstrated that the levels of inflammatory cells (Ly6G+/CD14+/CD68+/CD11b^{lo}/myeloperoxidase+) and albumin were lowest in group 1, highest in group 2, and significantly higher in groups 3 and 4 than in group 5 (all $P < 0.0001$), whereas arterial oxygen-saturation (SaO₂%) displayed an opposite pattern of albumin among the groups. Histopathological findings of lung injury/fibrosis area and inflammatory/DNA-damaged markers (CD68+/ γ -H2AX) displayed an identical pattern of SaO₂% among the groups (all $P < 0.0001$). The protein expressions of inflammatory (TLR-4/MMP-9/IL-1 β /TNF- α)/oxidative stress (NOX-1/NOX-2/p22phox/oxidized protein)/mitochondrial-damaged (cytosolic-cytochrome-C/dynamin-related protein 1)/autophagic (beclin-1/Atg-5/ratio of LC3B-II/LC3B-I) biomarkers exhibited a similar manner, whereas antioxidants [nuclear respiratory factor (Nrf)-1/Nrf-2]/cellular junctions (ZO-1/E-cadherin)/mitochondrial electron transport chain (complex I-V) exhibited an opposite manner of albumin among the groups (all $P < 0.0001$).

CONCLUSION

Combined EX^{AD}-mito^{Ex} therapy was better than merely one for protecting the lung against ARDS-SS induced injury.

Key Words: Acute respiratory distress syndrome; Sepsis syndrome; Exosomes; Mitochondria; Adipose tissue-derived mesenchymal stem cells; Inflammation

©The Author(s) 2024. Published by Baishideng Publishing Group Inc. All rights reserved.

Core Tip: To investigate whether combined adipose-derived mesenchymal-stem-cells-derived exosome (EX^{AD}) and exogenous mitochondria (mito^{Ex}) protect the lung from acute respiratory distress syndrome complicated by sepsis syndrome. The results of this study showed that combined EX^{AD} and mito^{Ex} exerted a synergic effect on protecting the lung from acute respiratory distress syndrome complicated by sepsis syndrome mainly by suppressing inflammatory reaction and oxidative stress, resulting in improved respiratory system and outcomes.

Citation: Lin KC, Fang WF, Yeh JN, Chiang JY, Chiang HJ, Shao PL, Sung PH, Yip HK. Outcomes of combined mitochondria and mesenchymal stem cells-derived exosome therapy in rat acute respiratory distress syndrome and sepsis. *World J Stem Cells* 2024; 16(6): 690-707

URL: <https://www.wjgnet.com/1948-0210/full/v16/i6/690.htm>

DOI: <https://dx.doi.org/10.4252/wjsc.v16.i6.690>

INTRODUCTION

Sepsis syndrome (SS), a systemic disease caused by overwhelming infections has been reported to occur in as many as three million adults in the United States annually, resulting in substantial morbidity and mortality[1]. On the other hand, acute respiratory distress syndrome (ARDS) is a devastating complication of SS. SS is one of the most common etiology of ARDS[2,3] and ARDS complicated by SS is associated with the highest case-fatality rate[2,4]. Universally, once ARDS develops, lung ventilatory support is the only intervention known to be improved mortality rates[5]. However, severe ARDS carries an extremely high mortality rate, and few effective therapeutic modalities exist to combat this condition[6-8].

Various cellular and molecular mechanisms are involved in the pathophysiologies of ARDS and SS[8-13]. Dysregulated inflammation is a pathophysiological features of ARDS-sepsis[8]. The pathways of innate immune responses are activated by toll-like receptors (TLRs) binding by either pathogen-associated molecular patterns or damage-associated molecular patterns that serve as danger signals. Activation of these TLRs leads to proinflammatory signaling, and robust production of cytokines and chemokines, activating alveolar macrophages and recruiting neutrophils from the vasculature into the alveolar space[14]. On the other hand, nucleotide-binding and oligomerization domain-like receptors can also be activated, leading to inflammasome activation, caspase-1 cleavage and release of the proinflammatory cytokines [*i.e.*, interleukin (IL)-1 and IL-18][14].

Adherent junction maintained the integrity of the lung endothelial barrier. Proinflammatory agonists, such as thrombin, vascular endothelial growth factor, tumor necrosis factor (TNF)- α , IL-1, and bacterial products [*i.e.*, lipopolysaccharide (LPS)] may increase pulmonary vascular permeability in ARDS-SS[15]. The alveolar epithelium is an important site of injury in ARDS-SS that contributes to enhance alveolar-capillary barrier destruction and its permeability and the formation of pulmonary edema[16]. Therefore, an aberrant host response to ARDS/ARDS-SS leads to the disruption of the pulmonary alveolar-capillary barrier, resulting in lung injury characterized by hypoxemia, inflammation, and pulmonary edema.

Our previous studies showed that exogenous mitochondrial delivery significantly protected the heart[17] and liver[18, 19] from ischemia-reperfusion (IR) injury, and effectively protected the lung from ARDS[9,13] and pulmonary arterial hypertension- induced lung injury[20] mainly by inhibiting excessive intracellular levels of reactive oxygen species, inflammation, and apoptosis as well as refreshment of mitochondria in ischemic organs. Accumulating evidence has shown that adipose derived mesenchymal stem cells (ADMSCs) have therapeutic potential ischemia-related organ dysfunction because of their pro-angiogenic, anti-inflammatory, and immunomodulatory properties against[11,21]. Exosomes, which are microvesicles derived from many kinds of cells, are membrane fragments with sizes ranging from 60-120 nm[22-24]. Depending on the cell type from which they are secreted, exosomes contain a rich collection of microRNAs, mRNA, DNA, and proteins[25]. Furthermore, previous studies have demonstrated that MSCs-derived exosomes have distinctive properties, including, promotion of angiogenesis, immunomodulation, and paracrine effects that preserve organ function following injury[26-29]. Interestingly, our recent studies revealed that ADMSCs-derived exosomes (EX^{AD}) treatment effectively attenuated IR injury in the brain, kidney, liver, and lung[24-27]. Additionally, it is well recognized that combined chemotherapy is frequently superior to merely one for suppressing the cancer cell growth and invasion *via* blocking the different mechanism of cancer cell proliferation. However, whether a combined regimen of exogenous mitochondria (mito^{Ex}) and exosomes would offer a synergistic effect in safeguarding the lungs from ARDS-induced damage is current remains unclear. Based on the above considerations, we hypothesized that combined EX^{AD} and mito^{Ex} may offer a synergic effect [*i.e.*, by inhibiting the inflammatory reaction, augmenting the immunomodulation by EX^{AD} and refreshing the adenosine triphosphate (ATP)/energy by transferring the mito^{Ex}] on protecting the lung functional integrity and its architecture against ARDS-SS injury.

MATERIALS AND METHODS

Ethical issues

Animal investigations were authorized by the Committee at Kaohsiung Chang Gung Memorial Hospital (Affidavit of Approval of Animal Use Protocol No. 2020121604) and performed in accordance with the Guide for the Care and Use of Laboratory Animals, 8th edition (NIH publication No. 85-23, National Academy Press, Washington, DC, United States, revised 2011). Animals were housed in American Association for Accreditation of Laboratory Animal Care-approved animal facility in our hospital, with controlled temperature and light cycles (24 °C and 12/12 light/dark cycle).

A rat model of ARDS complicated by SS and animal grouping

The procedures and protocols were based on our previous reports[9-11]. Briefly, the rats were placed in a sealed clear glass box with free access to food and water supply, and pure oxygen (100% O₂) was continuously administered for 48 h. After the inhalation of pure oxygen for 48 h, the ARDS model was created. This model was also validated by the previous studies[9-11]. Additionally, to mimic the clinical setting of ARDS complicated by SS (*i.e.*, ARDS-SS), the cecal ligation and puncture (CLP) was performed in the ARDS groups, 72 h after finishing ARDS induction. CLP was performed to induce sepsis as previously described[10,11]. The adult-male SD rats (Charles River Technology, BioLASCO Taiwan Co. Ltd., Taiwan) were used in our study and equally categorized into five groups: Group 1 [sham-operated control (SC), *i.e.*, only by opening the abdomen, followed by closure of the muscle and skin layers], group 2 (ARDS-SS), group 3 [ARDS-SS + EX^{AD} (100 μ g/rat)], group 4 [ARDS-SS + mito^{Ex} (1 mg/rat)] and group 5 (ARDS-SS + EX^{AD} + mito^{Ex}), respectively. The dosages of exosomes and mitochondria utilized in the present study were based on previous reports[9-11] (Supple-

mentary Figure 1).

Preparation of adipose tissue for ADMSCs

To isolate the adipose tissue for ADMSCs culture, an additional 12 rats (*i.e.*, served as the donors of ADMSCs for the preparation of exosomes) were utilized. Adipose tissues from the epididymis and abdominal areas were carefully isolated according to previous reports[10,11] by day 14 before exosome treatment. Cell culture was performed in Dulbecco's modified Eagle's medium-low glucose medium containing 10% fetal bovine serum (FBS) for at least fourteen days. Roughly, $(2.5-3.5) \times 10^7$ ADMSCs were obtained from each animal after 14-d cell culture.

Isolation of EX^{AD}

The procedure and protocol have been described in our previous reports[21,22]. Briefly, ADMSCs were grown in the presence of 10% exosome-depleted FBS (Thermo Fisher Scientific) and exosomes were harvested from this cell culture medium. Cells and debris were removed by centrifugation at $350 \times g$ for 10 min and $2000 \times g$ for 30 min, respectively. For precipitation, total exosome isolation kit (Thermo Fisher Scientific) was added to the cell and debris-free cell medium (1:2 with exosome isolation reagent and cell medium, respectively). Cell medium and the exosome isolation reagent were mixed by brief vortexing and incubated at 4 °C overnight before centrifuged at 4 °C, at $10000 \times g$ for 1 h. The pellet containing the pre-enriched exosomes was resuspended in phosphate-buffer saline.

Mitochondrial isolation

In the present study, six additional animals served as mitochondria donors. The procedures and protocols of liver mitochondrial isolation were based on our previous report[9]. In detail, the rats were starved overnight prior to mitochondrial isolation. The rats were then euthanized, and the livers were harvested. Immediately, the liver (3 g) was immersed into 50 cc of ice-cold isolation buffer (IBc) (10 mmol/L Tris-MOPS, 5 mmol/L EGTA/Tris and 200 mmol/L sucrose, pH = 7.4), followed by rinsing the liver free of blood by using ice-cold IBc. The liver was then minced into small pieces using scissors in a beaker surrounded by ice. The IBc was discarded during mincing and replaced with 18 mL of ice-cold fresh IBc. Livers were homogenized using a Teflon pestle. The homogenate was transferred to a 50 mL polypropylene Falcon tube and then centrifuged at $600 \times g$ for 10 min at 4 °C. The supernatants were again transferred to centrifuge tubes for centrifugation at $7000 \times g$ for 10 min at 4 °C. The supernatants were discarded, and the pellets were washed with 5 mL of ice-cold IBc. Again, the supernatants from pellets were centrifuged at $7000 \times g$ for 10 min at 4 °C. The supernatants were discarded, and the pellets containing mitochondria were resuspended. The concentration of the mitochondrial suspension was measured using the Biuret method. Mitochondrial transfusion was performed in the study animals immediately after preparation (*i.e.*, < 3 h post isolation).

Procedure and protocol for quantification of oxygen consumption rate of isolated mitochondria (Seahorse method)

The procedures and protocols were based on this previous report[9]. The functional activity of isolated mitochondria from the rat liver was determined by an Extracellular Flux Analyzer (XF24, Seahorse Bioscience, MA, United States) through measuring the degree of coupling between the electron transport chain (ETC) and oxidative phosphorylation (OXPHOS) machinery. Mitochondrial bioenergetics as reflected in the integrity of the ETC and capacity of OXPHOS were evaluated by measuring the mitochondrial oxygen consumption rate (OCR). In this study, isolated mitochondria (10 µg/well) from rat liver were diluted in cold 1× mitochondria assay solution (70 mmol/L sucrose, 220 mmol/L mannitol, 10 mmol/L KH₂PO₄, 5 mmol/L MgCl₂, 2 mmol/L HEPES, 1.0 mmol/L EGTA and pH = 7.2), followed by spinning down at $3000 \times g$ for 30 min. After attachment of mitochondria to the XF24 plate, the coupling reaction was initiated by administering the substrate (10.0 mmol/L succinate). State 3 was initiated with ADP (0.5 mmol/L), while state 4 was induced with the addition of oligomycin (2 µmol/L). Maximal uncoupler-stimulated respiration was elicited with carbonyl cyanide-p-trifluoromethoxyphenylhydrazone (FCCP) (4 µmol/L), whereas complex III repression was induced by antimycin A (4 µmol/L). The mitochondrial OCR in reactions mentioned above was sequentially measured.

Histological findings of lung injury

The lung injury score assessment was based on our previous report[21]. Briefly, lung specimens were sectioned at 5 µm for light microscopy. Hematoxylin and eosin (H&E) staining was carried out to assess the number of alveolar sacs. Three lung sections from each rat were analyzed; three randomly selected high-power fields (HPFs; 100 ×) were examined in each section, and the mean number was determined. The extent of the crowded area, which was defined as regions of thickened septa in the lung parenchyma associated with partial or complete collapse of alveoli on H&E-stained sections, was also assessed in a blinded manner. The following scoring system was adopted: (1) 0, no detectable crowded area in a given HPF; (2) 1, < 15% crowded area; (3) 2, 16%-25%; (4) 3, 26%-50%; (5) 4, 51%-75%; and (6) 5, > 75%.

Western blot analysis

Equal amounts (50 µg) of protein extracts were separated by sodium-dodecyl sulfate gel electrophoresis. After electrophoresis, the separated proteins were transferred onto a polyvinylidene difluoride membrane (Amersham Biosciences). Nonspecific sites were blocked with blocking buffer [5% nonfat dry milk in TBS containing 0.05% Tween 20 (T-TBS)] for 1 h at room temperature. Membranes were incubated with the indicated primary antibodies [cytosolic cytochrome C (1:1000, BD), NOX-1 (1:2000, Sigma-Aldrich), NOX-2 (1:500, Sigma-Aldrich), p22phox (1:1,000, Abcam), total OXPHOS antibody cocktail (1:1,000, Abcam), dynamin-related protein (DRP) 1 (1:1,000, cell signaling), mitofusin-2 (Mfn2) (1:1000, cell signaling), peroxisome proliferator-activated receptor gamma coactivator 1-alpha, nuclear respiratory factor 1 (NRF1) (1:1000, cell signaling), NRF2 (1:1000, Abcam), beclin-1 (1:1000, cell signaling), autophagy related 5 (Atg5) (1:1000, cell

signaling), LC3B-I/II (1:2000, Abcam), and β -actin (1:10000, Chemicon)] overnight at room temperature. The membranes were then incubated with a secondary antibody, horseradish peroxidase-conjugated anti-rabbit immunoglobulin IgG (1:2000, cell signaling), for 1 h at room temperature. The washing procedure was repeated eight times within 1 h. Immunoreactive bands were visualized using enhanced chemiluminescence (ECL; Amersham Biosciences) and exposed to Biomax L film (Kodak). For quantification, ECL signals were digitized using the Labwork software (UVP).

Immunohistochemical and immunofluorescent staining

The procedures and protocols were based on our previous reports[9,11,13]. Rehydrated paraffin sections were treated with 3% H₂O₂ for 30 min., and then incubated with Immuno-Block reagent (BioSB) for 30 min at room temperature. Sections were incubated with primary antibodies against zonula occludens 1 (ZO-1) (1:200, Thermo Fisher Scientific), E-cadherin (1:200, Thermo Fisher Scientific), occluding (1:200, Thermo Fisher Scientific), claudin (1:200, Thermo Fisher Scientific), F4/80+ (1:250, Cell Signaling Technology), CD40L+ (1:200, Thermo Fisher Scientific), CD14 (1:200, BioSS), CD68 (1:100, Abcam), CD31 (1:100, Abcam), heme-oxygenase-1 (1:250, Abcam), and glutathione reductase (1:300, Abcam), while sections incubated with irrelevant antibodies served as controls. Three lung sections from three rat were analyzed. For quantification, three randomly selected HPFs (200 × or 400 × magnification) were analyzed in each section. The mean number of positively stained cells per HPF for each animal was then determined by the summation of all numbers divided by 9.

Mitochondrial DNA copy number in lung parenchyma

Total DNA was extracted from the lung parenchyma using the DNeasy Blood and Tissue kit (Qiagen) with proteinase K and RNase treatment, according to the manufacturer's instructions. The copy number of mitochondrial DNA (mitDNA) was quantified by QuantiNOVA SYBR Green PCR assay (Qiagen) and normalized by rat genomic GAPDH DNA. Primer sequences are listed below: ND1 - mtDNA forward: 5'-CTCCCTATTCGGAGCCCTAC-3'; ND1 - mtDNA reverse: 5'-ATTGTCTTCTGCTAGGGTTG-3'; GAPDH - DNA forward: 5'-GTTACCAGGGCTGCCTTCTC-3'; GAPDH - DNA reverse: 5'-GGGTTTCCCGTTGATGACC-3'; ANP forward: 5'-CTGCTAGACCACCTGGAGGA-3'; ANP reverse: 5'-AAGCTGTTGCAGCCTAGTCC-3'[17]. Triplicate assays were performed for each sample using Step One-Plus system (Applied Biosystems).

Statistical analysis

Quantitative data were expressed as mean \pm SD. Statistical analysis was conducted using ANOVA followed by Bonferroni multiple-comparison *post hoc* test. The SAS statistical software for Windows version 8.2 (SAS Institute, Cary, NC, United States) was utilized. Statistical significance was set at $P < 0.05$.

RESULTS

Qualitative exosome biomarkers and OCR of mitochondria

To verify the specific biomarkers of exosomes, the western blot analysis was performed. The result showed that the protein expressions of CD63, TSG101 and β -catenin, three specific biomarkers of exosomes, were notably increased as the concentration of exosomes was stepwise increased from 1 μ g, 2 μ g, 10 μ g, to 50 μ g, particularly increased in the 50- μ g concentration of the sample (Figure 1A).

Additionally, to verify the OCR of isolated mitochondria (*i.e.*, the time courses of mitochondrial respiration and glycolysis), the Seahorse assay was utilized (*i.e.*, using Seahorse XF Analyzers to measure the OCR) for several different situations, including the injection of oligomycin, FCCP, and antimycin A/rotenone. The results showed that mitochondrial respiration reflected by the level of OCR was remarkably high, implicating that the isolated mitochondrial had excellent functional integrity and efficacy (Figure 1B).

Influence of mito^{Ex} transfusion into L2 cells

To clarify whether mito^{Ex} could be transfused into the recipient cells, the L2 cells were categorized into groups A1 (*i.e.*, L2 cell only), A2 [L2 cells + (hypoxia condition: O₂ 1%, CO₂ 5%, other N₂ for 3 h)], A3 [L2 cells + exogenous mitochondrial (100 μ g) mixed with cells for 24 h] and A4 (L2 cells + hypoxia for 3 h, followed by mixture of mito^{Ex} with the cells for 24 h), respectively. The result of immunofluorescent (IF) microscopic examination (Figure 2A-C) showed that the mitochondria in the L2 cells [*i.e.*, the intracellular level of endogenous mitochondria (Figure 2D) and total mitochondria, *i.e.*, summation of endogenous + mito^{Ex} (Figure 2E)] were lowest in A2, highest in A4 and significantly higher in A3 than in A1. Additionally, the quantitative polymerase chain reaction demonstrated that the relative mitDNA exhibited a similar pattern of IF microscopic finding among the groups (Figure 3A). Furthermore, the concentration level of ATP exhibited a comparable pattern of mitDNA among the groups (Figure 3B). These findings implicated that the mito^{Ex} were quite easily transfused into the recipient cells, especially under condition of hypoxia (*i.e.*, implicated damaged mitochondrial cells).

To elucidate whether exogenous mitochondrial transfusion into L2 cells would augment the expressions of tight junctions protein in pulmonary epithelial cells, the western blot analysis was utilized. The results of western blot analysis demonstrated that the protein expressions of occluding (Figure 3C), ZO-1 (Figure 3D), β -catenin (Figure 3E) and E-cadherin (Figure 3F), four indicators of pulmonary epithelial cellular junctions for assessment of pulmonary epithelial integrity, also exhibited an identical pattern of IF microscopic finding among the groups (Figure 2D and E).

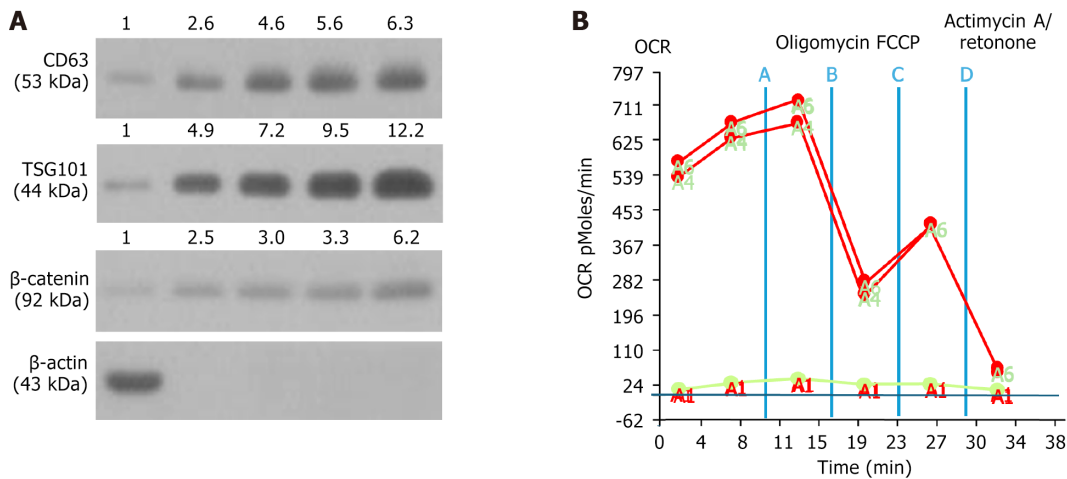


Figure 1 Qualitative exosome biomarkers and oxygen consumption rate of mitochondria. A: Illustrating the protein expressions of CD63, TSG101 and β -catenin. The result showed that the protein expressions of these three fundamental biomarkers of exosome were notably progressively increased as the concentration of exosomes was stepwise increased from 1 μ g, 2 μ g, 10 μ g, to 50 μ g; B: Illustrating the oxygen consumption rate (OCR) curve; the result showed that the mitochondrial respiration reflected by the level of OCR was remarkably high, implicating that the isolated mitochondria had excellent functional integrity and efficacy. A: Untreated; B: Oligomycin; C: Carbonyl cyanide-p-trifluoromethoxyphenylhydrazone; D: Actinomycin A/rotenone. OCR: Oxygen consumption rate; FCCP: Carbonyl cyanide-p-trifluoromethoxyphenylhydrazone.

Exosomes suppressed inflammation/oxidative stress and preserved cell junctions

To elucidate whether the exosome treatment would attenuate the inflammatory reaction, the L2 cells were categorized into B1 (L2 cells), B2 [L2 cells + LPS (1.0 μ g/mL)], and B3 [L2 cells + LPS (1.0 μ g/mL) + exosomes (100 μ g)] groups, respectively. The result showed that the protein expressions of IL-1 β (Figure 4A), TNF- α (Figure 4B), nuclear factor- κ B (Figure 4C), TLR-4 (Figure 4D) and matrix-metalloproteinase-9 (Figure 4E), five indicators of inflammation, were significantly higher in B2 than in B1 that were significantly reversed in B3. Additionally, the protein expressions of NOX-1 (Figure 4F) and NOX-2 (Figure 4G), two indicators of oxidative stress, and protein expressions of cleaved caspase 3 (Figure 4H) and cleaved poly (ADP-ribose) polymerase (Figure 4I), two indices of apoptosis, exhibited an identical manner of inflammation among the groups.

Furthermore, to verify whether the pulmonary epithelial cell-cell junctions would also be affected by LPS-exosome treatment, the western blot analysis was utilized again. As we expected, the protein expressions of occluding (Figure 4J), β -catenin (Figure 4K), ZO-1 (Figure 4L) and E-cadherin (Figure 4M), four indicators of pulmonary epithelial cellular junctions, exhibited an opposite pattern of inflammation among the three groups.

Inflammation/albumin in bronchoalveolar lavage fluid and circulatory cytokines and mortality

To elucidate the therapeutic effect of EX^{AD}-mito^{Ex} on lung protection against ARDS-SS injury, flow cytometric analysis of bronchoalveolar lavage (BAL) fluid was conducted by day 5 after ARDS induction. The result showed that the BAL fluid level of TNF- α (Figure 5A), a proinflammatory cytokine, was highest in group 2 (ARDS-SS), lowest in SC, significantly higher in group 4 (ARDS-SS + mito^{Ex}) than in group 3 (ARDS-SS + EX^{AD}) and group 5 (ARDS-SS + EX^{AD} + mito^{Ex}) and significantly higher in group 3 than in group 5. Additionally, circulating numbers of Ly6G⁺ (Figure 5B), CD11^{b/c+} (Figure 5C) and myeloperoxidase⁺ (Figure 5D) cells, three indicators of inflammatory cells, exhibited an identical pattern of TNF- α among the groups.

Furthermore, the albumin level in the BAL fluid, an indicator of increased permeability and leakage in the lung parenchyma after ARDS-induced damage, was lowest in group 1 and significantly and progressively reduced in groups 2 to 5. On the other hand, the relative mitDNA (Figure 5E) level in the lung tissue was lowest in group 2, highest in group 5, significantly higher in group 4 than in groups 1 and 3, and significantly higher in group 1 than in group 3.

Moreover, the circulatory levels of TNF- α (Figure 5F) and IL-6 (Figure 5G), two indices of proinflammatory cytokine, exhibited an identical pattern of Ly6G in BAL fluid among the groups. Our findings suggested that combined exosome and exogenous mitochondrial therapy was better than merely one for alleviating the inflammatory reaction. A total of 121 rats were utilized in the present study and the aim of this study proposed that at the end of the study period, the numbers of the survival animals in each group should be more than 10 for individual study. Additionally, we prospectively randomized the animals into different groups immediately after completely ARDS induction.

Prior to categorizing the animals into different groups, the mortality rate was 28.9% (35/121). However, after grouping (*i.e.*, during the treatment period), the mortality rates were 0%, 44.0% (11/25), 23.5% (4/17), 17.7% (3/17) and 18.8% (3/16) in groups 1 to 5, respectively. Thus, the mortality rate at the end of the study period was significantly higher in group 2 than in group 1 (*i.e.*, $P < 0.049$) (Figure 5H). However, there was no significant difference between the groups 1 and 3 to 5 or between the groups 2 to 5 ($P > 0.1$). To elucidate the severity of lung parenchymal leakage in ARDS, albumin levels in BAL fluid were analyzed in the current study. The results demonstrated that this parameter expressed an identical pattern of circulatory levels of inflammatory cells among the groups (Figure 5I).

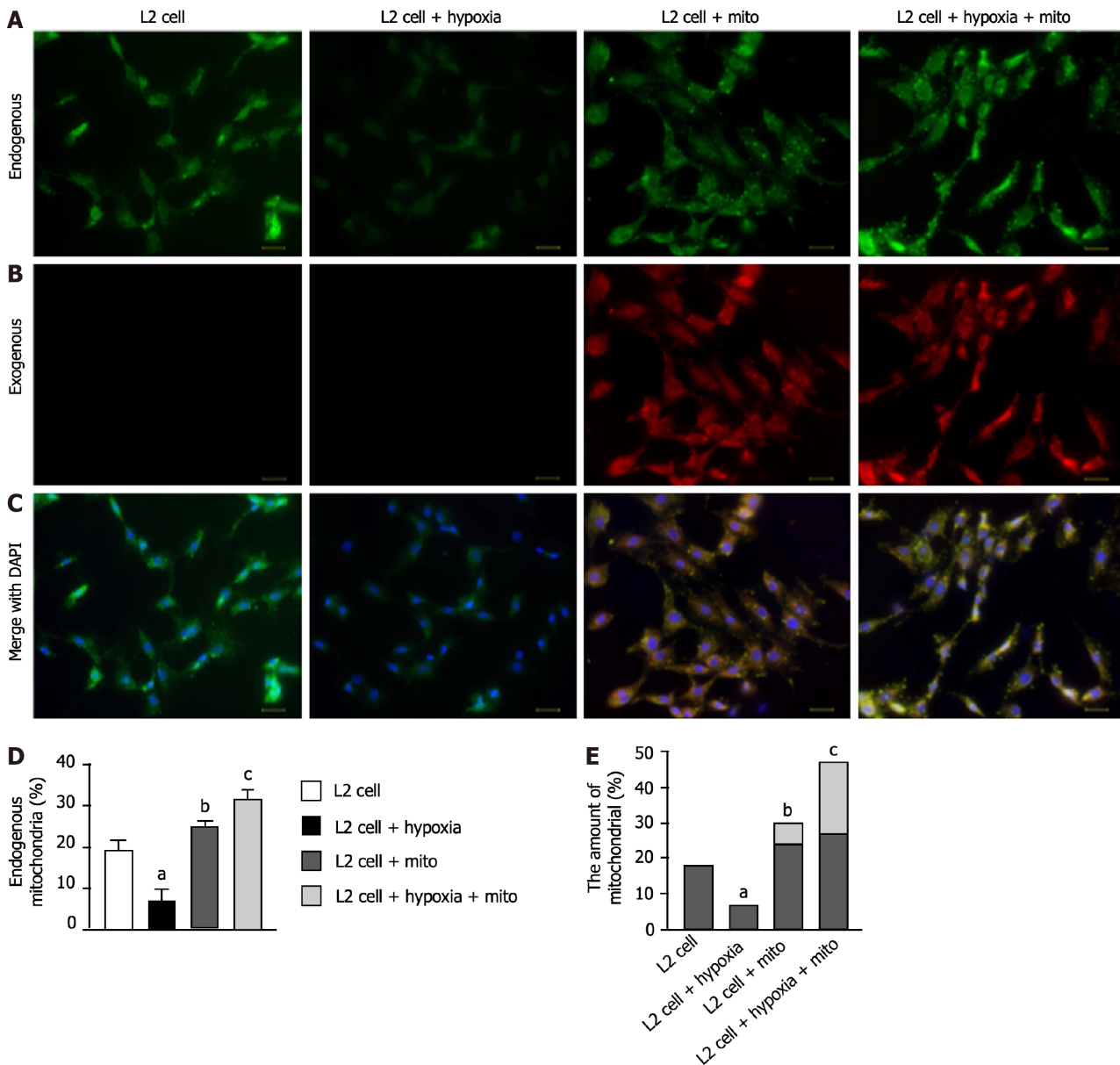


Figure 2 Immunofluorescent microscopic finding for elucidating the ability of exogenous mitochondria transfusion into the L2 cells. A: Demonstrating MitoTracker stain (400 ×) for identifying endogenous mitochondria (green color) among four groups; B: Indicating the MitoTracker stain (400 ×) for identifying exogenous mitochondria to be transfused into the L2 cells (red color); C: Denoting the merged picture of a4 to b4 (*i.e.*, endogenous and exogenous mitochondrial staining). Pink-yellow color indicated the endogenous and exogenous mitochondria colocalized together. Abundant mitochondria were found in c3 and c4 groups. Blue color in c1 to c4 indicated the DAPI stain (400 ×) for identifying rat lung epithelial cells (*i.e.*, L2 cell line) in four groups. Scale bars in right lower corner represent 20 μm; D: Analytical result of endogenous mitochondrial expression (%); E: Analytical result of combined expression of endogenous and exogenous mitochondrial amount. Dark bar chart indicated percentage of endogenous mitochondria, whereas gray color indicated percentage of exogenous mitochondria. All statistical analyses were performed by one-way ANOVA, followed by Bonferroni multiple comparison *post hoc* test ($n = 5$ for each group). Control vs other groups with different letters, ^a $P < 0.01$, ^b $P < 0.05$, ^c $P < 0.001$. Grouping: L2 cells; L2 cells + hypoxia; L2 cells + mitochondria (100 μg); L2 cells + hypoxia + mitochondria (100 μg).

Oxidative stress, autophagy and DNA-damaged markers post-5-d ARDS induction

It is well known that the oxidative stress and autophagy play an essential role in lung parenchymal damage after acute lung injury. Therefore, western blot analysis was utilized for these parameters. The protein expressions of NOX-1 (Figure 6A) and NOX-2 (Figure 6B), two indices of oxidative stress, were highest in group 2, lowest in group 1 and significantly lower in group 5 than in groups 3 and 4, but were similar between groups 3 and 4. In contrast, the protein expressions of Nrf1 (Figure 6C) and Nrf2 (Figure 6D), two indicators of anti-oxidants, exhibited an opposite pattern of oxidative stress among the groups.

The protein expression of beclin-1 (Figure 6E), Atg5 (Figure 6F) and the ratio of LC3B-II to LC3B-I (Figure 6G), three indicators of autophagy, displayed an identical pattern of oxidative stress among the groups. Additionally, the cellular level of γ -2AX, an index of DNA damage, showed a similar manner of autophagy (Figure 6H-M). Our findings suggested that combined exosome and exogenous mitochondrial therapy was superior to just one for ameliorating the oxidative stress, autophagy and DNA damage.

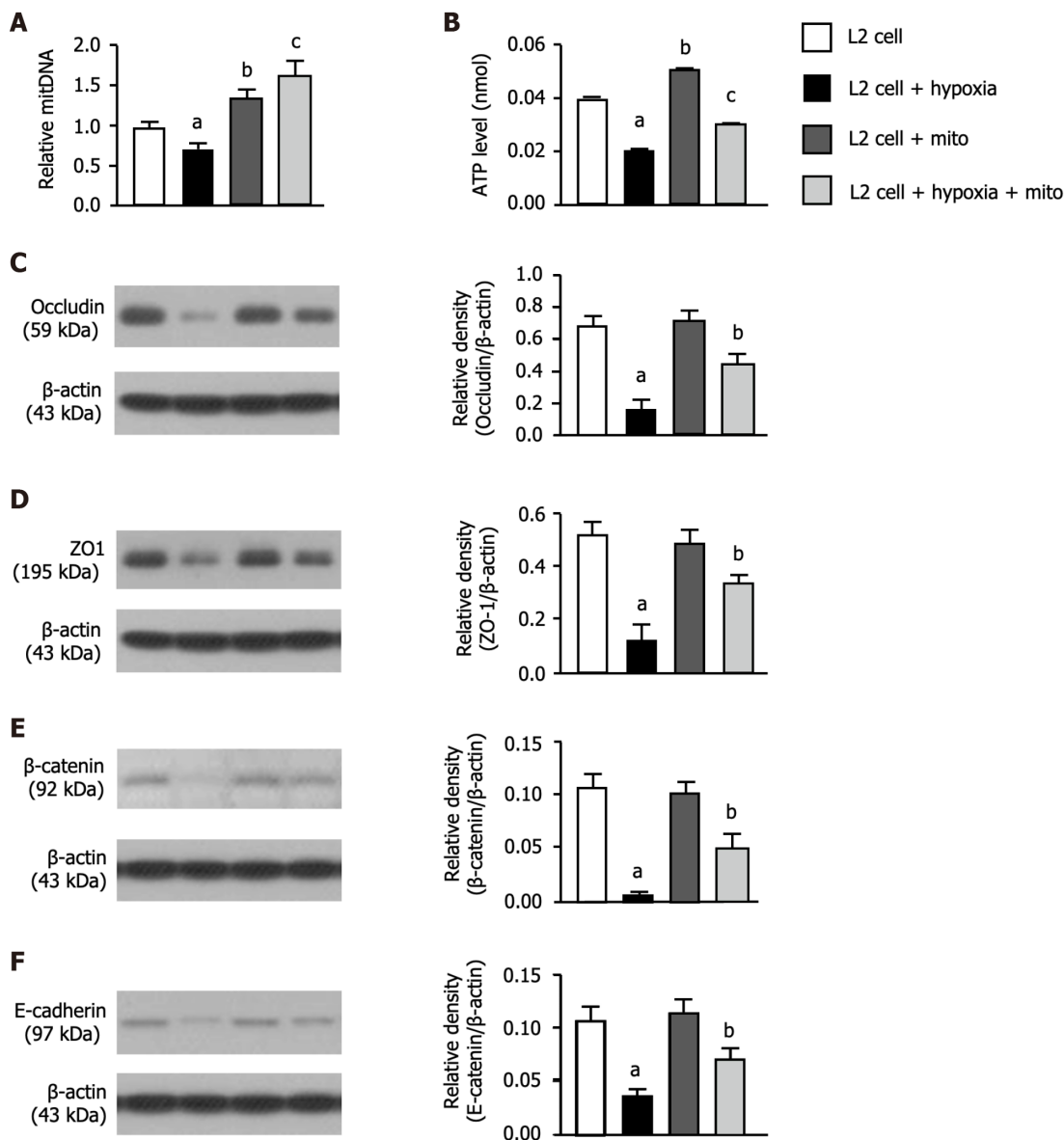


Figure 3 Protein expressions of cellular junctions, relative mitochondrial DNA expression and adenosine triphosphate concentration. A: Relative mitochondrial DNA expression, control vs other groups with different letters, ^a $P < 0.01$, ^b $P < 0.05$, ^c $P < 0.001$ ($n = 6$ for each group); B: Concentration level of adenosine triphosphate, control vs other groups with different letters, ^a $P < 0.01$, ^b $P < 0.05$, ^c $P < 0.001$ ($n = 6$ for each group); C: Protein expression of occludin, control vs other groups with different symbols, ^a $P < 0.001$, ^b $P < 0.01$; D: Protein expression of β -catenin, control vs other groups with different letters, ^a $P < 0.001$, ^b $P < 0.01$; E: Protein expression of zonula occludens-1, control vs other groups with different letters, ^a $P < 0.001$, ^b $P < 0.01$; F: Protein expression of E-cadherin, control vs other groups with different letters, ^a $P < 0.001$, ^b $P < 0.01$ ($n = 4$ for each group). All statistical analyses were performed by one-way ANOVA, followed by Bonferroni multiple comparison *post hoc* test. Grouping: L2 cells; L2 cells + hypoxia; L2 cells + mitochondria (100 μ g); L2 cells + hypoxia + mitochondria (100 μ g).

Mitochondrial damaged markers and cell junctions post-5-d ARDS induction

In order to realize the degree of mitochondria and cellular junctions damage, the western blot analysis was conducted. The protein expressions of DRP1 (Figure 7A), p22phox (Figure 7B) and cytosolic cytochrome C (Figure 7C), three indices of mitochondrial damaged markers, were lowest in group 1, highest in group 2, significantly lower in group 5 than in groups 3 and 4, however they showed similar between groups 3 and 4. Additionally, the protein expressions of ZO-1 (Figure 7D) and E-cadherin (Figure 7E), two indicators of cellular junctions of lung epithelial integrity, displayed an opposite pattern of the mitochondrial damaged markers. Our findings implied that combined exosome and mito^{Ex} therapy rescued the lung ultrastructural integrity against ARDS-SS damage.

ETC complexes, mfn and oxidative stress post-5-d ARDS induction

Next, we utilized the western blot analysis once more to determine the ETC and mitochondrial fusion. The result demonstrated that the protein expressions of complexes I-V (Figure 8A-E), five parameters of mitochondrial ETC, and the protein expression of Mfn2 (Figure 8F), an indicator of mitochondrial fusion, were highest in group 1, lowest in group 2, significantly higher in group 5 than in groups 3 and 4, but these parameters did not differ between groups 3 and 4, whereas the cellular level of oxidative stress (*i.e.*, 8-hydroxy-2'-deoxyguanosine stain) displayed an opposite manner of

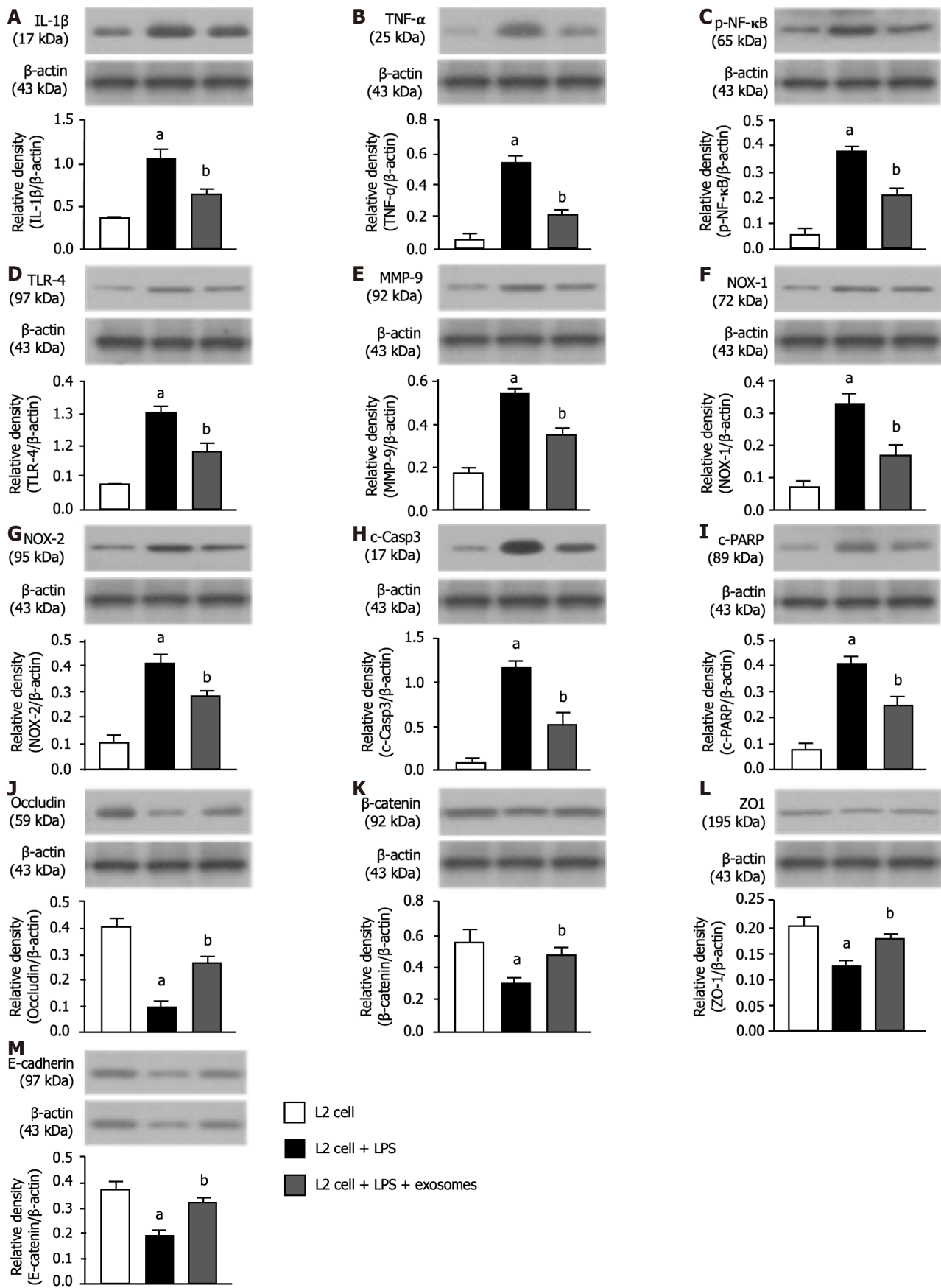


Figure 4 Exosomes therapy effectively reduced inflammation, oxidative stress and apoptosis and preserved the lung epithelial cell junctions. A: Protein expression of interleukin-1β; B: Protein expression of tumor necrosis factor-α; C: Protein expression of nuclear factor-κB; D: Protein expression of toll-like receptor-4; E: Protein expression of matrix metalloproteinase-9; F: Protein expression of NOX-1; G: Protein expression of NOX-2; H: Protein expression of cleaved caspase 3; I: Protein expression of cleaved poly (ADP-ribose) polymerase; J: Protein expression of occludin; K: Protein expression of β-

catenin; L: Protein expression of zonula occludens-1; M: Protein expression of E-cadherin. All statistical analyses were performed by one-way ANOVA, followed by Bonferroni multiple comparison *post hoc* test ($n = 3$ for each group). Control vs other groups with different letters, ^a $P < 0.001$, ^b $P < 0.01$. B1: L2 cells only; B2: L2 cells + lipopolysaccharide (LPS) (1.0 $\mu\text{g}/\text{mL}$); B3: L2 cells + LPS (1.0 $\mu\text{g}/\text{mL}$) + exosomes (10 μg). IL: Interleukin; TNF: Tumor necrosis factor; NF- κB : Nuclear factor NF- κB ; TLR: Toll-like receptor; MMP: Matrix metalloproteinase; c-Casp3: Cleaved caspase 3; ZO-1: Zonula occludens-1; PARP: Poly (ADP-ribose) polymerase; LPS: lipopolysaccharide.

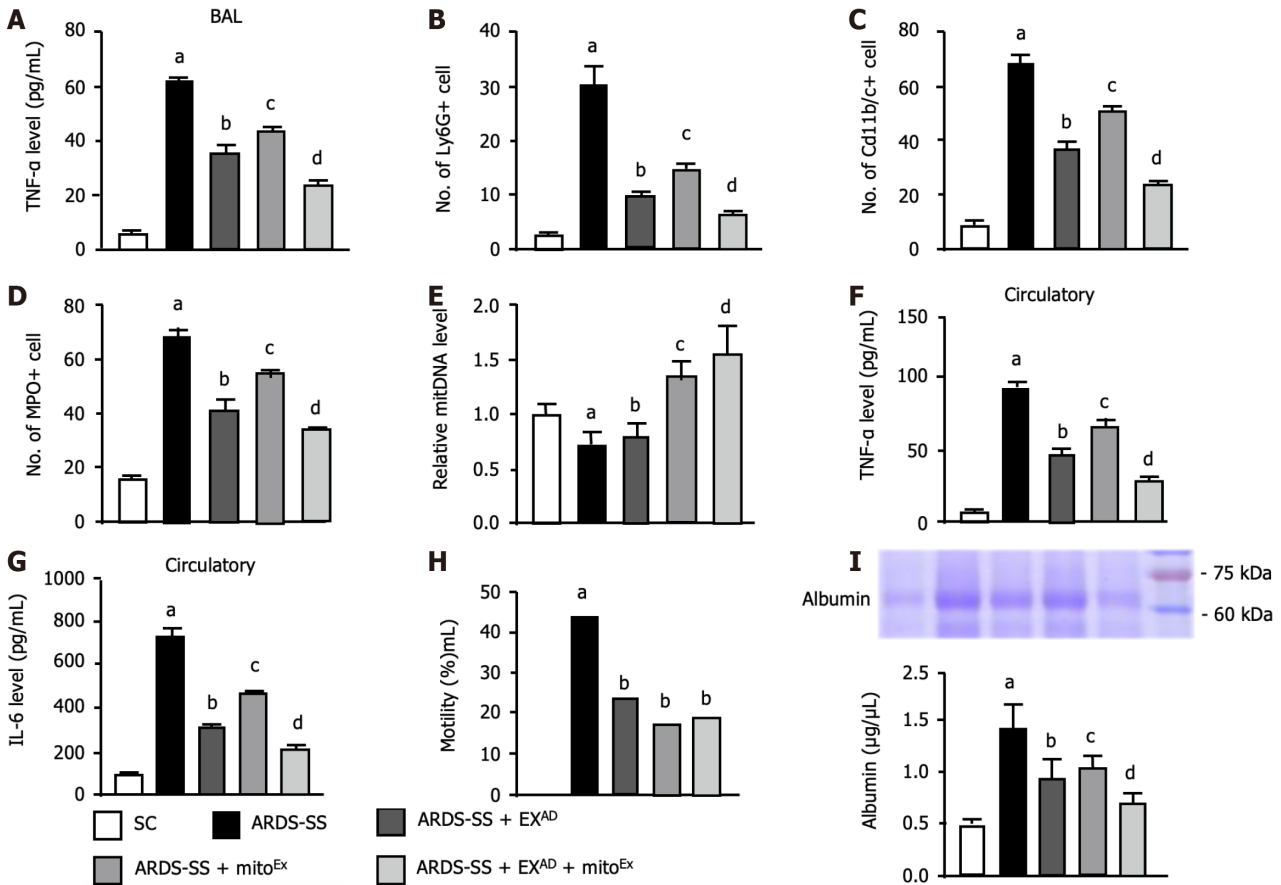


Figure 5 Levels of inflammatory cells and albumin in bronchoalveolar lavage fluid and circulatory proinflammatory cytokine by day 5 after acute respiratory distress syndrome induction. A: Enzyme-linked immunosorbent assay analysis of tumor necrosis factor (TNF)- α level in bronchoalveolar lavage (BAL), control vs other groups with different letters, ^a $P < 0.0001$, ^b $P < 0.01$, ^c $P < 0.05$, ^d $P < 0.001$; B: Flow cytometric analysis of number of Ly6G+ cells, control vs other groups with different letters, ^a $P < 0.0001$, ^b $P < 0.01$, ^c $P < 0.05$, ^d $P < 0.001$; C: Flow cytometric analysis of number of CD11b⁺c⁺ cells, control vs other groups with different letters, ^a $P < 0.0001$, ^b $P < 0.01$, ^c $P < 0.05$, ^d $P < 0.001$; D: Flow cytometric analysis of number of myeloperoxidase+ cells, control vs other groups with different letters, ^a $P < 0.0001$, ^b $P < 0.01$, ^c $P < 0.05$, ^d $P < 0.001$; E: Relative mitochondrial DNA level, control vs other groups with different letters, ^a $P < 0.01$, ^b $P < 0.05$, ^c $P < 0.001$, ^d $P < 0.0001$; F: Circulatory level of TNF- α , control vs other groups with different letters, ^a $P < 0.0001$, ^b $P < 0.05$, ^c $P < 0.01$, ^d $P < 0.001$; G: Circulatory level of interleukin-6, control vs other groups with different letters, ^a $P < 0.0001$, ^b $P < 0.05$, ^c $P < 0.01$, ^d $P < 0.001$; H: The mortality rate by day 5 after acute respiratory distress syndrome induction, control vs ^a $P < 0.05$, control vs ^b $P > 0.05$; I: Analytical result of BAL albumin concentration, control vs other groups with different letters, ^a $P < 0.0001$, ^b $P < 0.01$, ^c $P < 0.05$, ^d $P < 0.001$. All statistical analyses were performed by one-way ANOVA, followed by Bonferroni multiple comparison *post hoc* test ($n = 6$ for each group). IL: Interleukin; TNF: Tumor necrosis factor; MPO: Myeloperoxidase; SC: Sham-operated control; ARDS: Acute respiratory distress syndrome; SS: Sepsis syndrome; mito^{Ex}: Exogenous mitochondria; EX^{AD}: Adipose-derived mesenchymal stem cells-derived exosomes; BAL: Bronchoalveolar lavage.

ETC among the groups (Figure 8G-L), implicating that combined exosome and mito^{Ex} therapy was better than one therapy alone in protecting the cell mitochondrial homeostasis and effective energy utilization.

EX^{AD}-mito^{Ex} were identified in the lung parenchyma of ARDS rat

To delineate the final destination of EX^{AD} and mito^{Ex}, these two molecules were stained with specific dyes and serial sections of the lung (Figure 9), brain, heart, liver and kidney (Supplementary Figure 2) were investigated. IF microscopic findings demonstrated that the presence of EX^{AD} and mito^{Ex} could be identified only in lung specimens (Figure 9A-D). This study might support that only damaged lung organs could trap EX^{AD} and mito^{Ex} to safeguard the lung from ARDS damage.

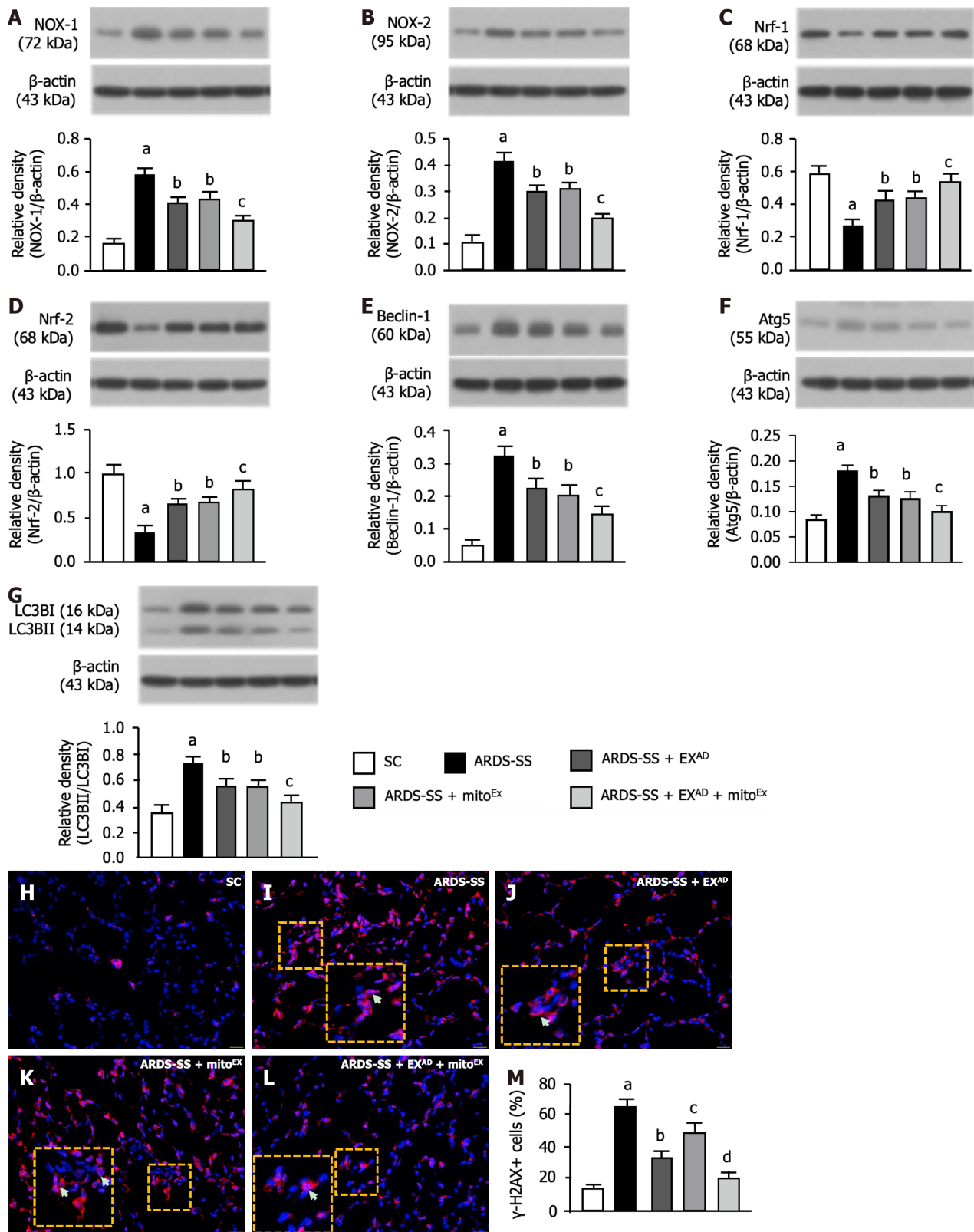


Figure 6 Protein expressions of oxidative stress and autophagy, and cellular level of DNA damage by day 5 after acute respiratory distress syndrome induction. A: Protein expression of NOX-1, control vs other groups with different letters, ^a*P* < 0.0001, ^b*P* < 0.05, ^c*P* < 0.01; B: Protein expression of NOX-2, control vs other groups with different letters, ^a*P* < 0.0001, ^b*P* < 0.05, ^c*P* < 0.01; C: Protein expression of nuclear respiratory factor 1 (Nrf1), control vs other groups with different letters, ^a*P* < 0.0001, ^b*P* < 0.05, ^c*P* < 0.01; D: Protein expression of Nrf2, control vs other groups with different letters, ^a*P* < 0.0001, ^b*P* < 0.05, ^c*P* < 0.01; E: Protein expression of beclin-1, control vs other groups with different letters, ^a*P* < 0.0001, ^b*P* < 0.05, ^c*P* < 0.01; F: Protein expression of autophagy related 5, control vs other groups with different letters, ^a*P* < 0.0001, ^b*P* < 0.05, ^c*P* < 0.01; G: Protein expression of the ratio of LC3B-II to LC3B-I, control vs other groups with different letters, ^a*P* < 0.0001, ^b*P* < 0.05, ^c*P* < 0.01; H-L: Illustrating the immunofluorescent microscopic finding (400 \times) for identification of γ -H2AX+ cells (red color). Yellow dotted line large square box was the manifestation of yellow dotted line small square box for more clear identification of double stained (*i.e.*, DAPI stain for nuclei+ γ -H2AX) γ -H2AX+ cells (white arrows). The scale bars in right lower corner represent 20 μ m; M: Analytical result of number of γ -H2AX+ cells,

control vs other groups with different letters, ^a*P* < 0.0001, ^b*P* < 0.01, ^c*P* < 0.05, ^d*P* < 0.001. All statistical analyses were performed by one-way ANOVA, followed by Bonferroni multiple comparison post hoc test (*n* = 6 for each group). Nrf1: Nuclear respiratory factor 1; Atg5: Autophagy related 5; SC: Sham-operated control; ARDS: Acute respiratory distress syndrome; SS: Sepsis syndrome; mito^{Ex}: Exogenous mitochondria; EX^{AD}: Adipose-derived mesenchymal stem cells-derived exosomes.

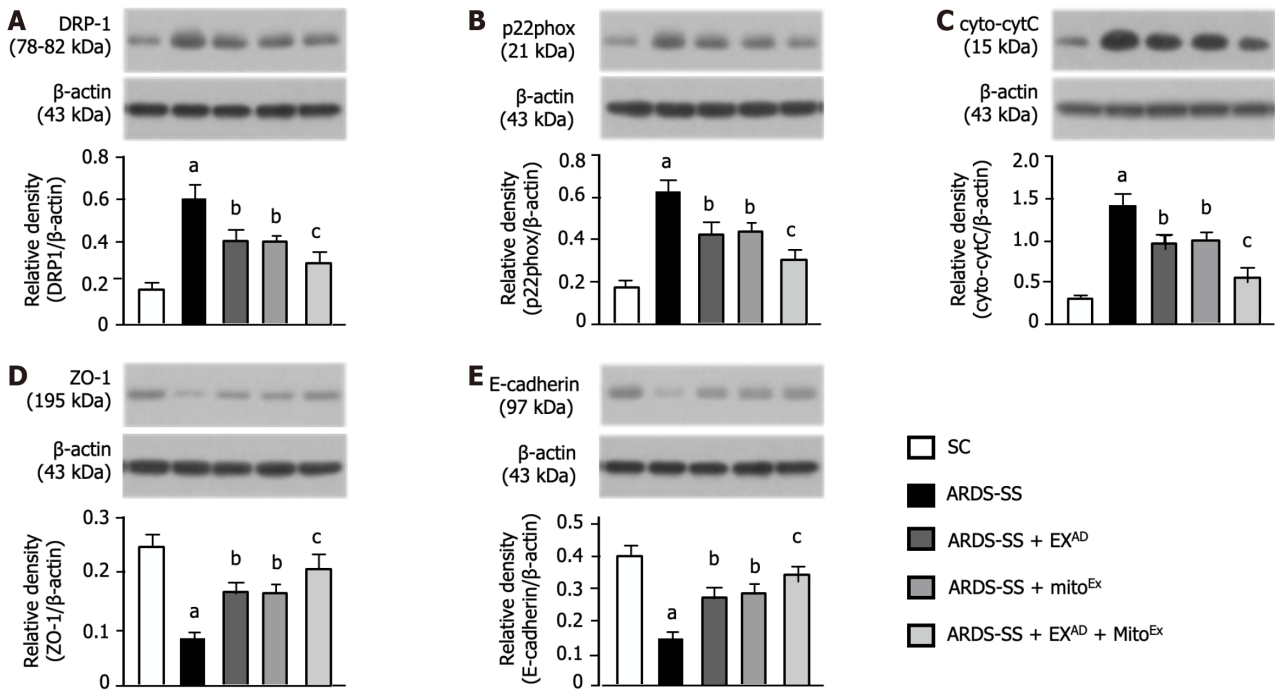


Figure 7 Protein expressions of mitochondrial damaged markers and cellular junctions by day 5 after acute respiratory distress syndrome induction. A: Protein expression of dynamin- related protein 1, control vs other groups with different letters, ^a*P* < 0.0001, ^b*P* < 0.05, ^c*P* < 0.01; B: Protein expression of p22phox, control vs other groups with different letters, ^a*P* < 0.0001, ^b*P* < 0.05, ^c*P* < 0.01; C: Protein expression of cytosolic cytochrome C, control vs other groups with different letters, ^a*P* < 0.0001, ^b*P* < 0.05, ^c*P* < 0.01; D: Protein expression of zonula occludens-1, control vs other groups with different letters, ^a*P* < 0.0001, ^b*P* < 0.05, ^c*P* < 0.01; E: Protein expression of E-cadherin, control vs other groups with different letters, ^a*P* < 0.0001, ^b*P* < 0.05, ^c*P* < 0.01. All statistical analyses were performed by one-way ANOVA, followed by Bonferroni multiple comparison post hoc test (*n* = 6 for each group). Drp1: Dynamin-related protein 1; cyto-CytC: Cytosolic cytochrome C; ZO-1: Zonula occludens-1; SC: Sham-operated control; ARDS: Acute respiratory distress syndrome; SS: Sepsis syndrome; mito^{Ex}: Exogenous mitochondria; EX^{AD}: Adipose-derived mesenchymal stem cells-derived exosomes.

Lung injury score and oxygen saturation (SaO₂%) post-5-d ARDS induction

To verify whether exosome and exogenous mitochondrial therapy would protect the cellular level of the lung parenchyma against ARDS-SS, microscopic findings of H&E staining (Figure 10A-E) were conducted. The results showed that the crowded score (Figure 10G), an indicator of histopathological finding of lung damage, was highest in group 2, lowest in group 1, significantly lower in group 5 than in groups 3 and 4, and notably lower in group 3 than in group 4. The number of alveolar sacs (Figure 10F) and SaO₂% (Figure 10H) exhibited the opposite pattern of crowded score among the groups. These findings implicated that combined exosome and mito^{Ex} therapy was better than either one for alleviating the lung injury score and preserving the lung functional integrity.

Cellular levels of fibrosis and inflammation post-5-d ARDS induction

Furthermore, to clarify the cellular levels of fibrosis and inflammatory expression, both IF and immunohistochemical microscopic findings were utilized for these studies. Masson’s trichrome staining (Figure 11A-E) demonstrated that the fibrotic area (Figure 11F) in the lung section was highest in group 2, lowest in group 1, significantly lower in group 5 than in groups 3 and 4 and notably lower in group 3 than in group 4. Additionally, the cellular expression of CD68+ cells (Figure 11G-K), an indicator of inflammation, expressed an identical manner of fibrosis among the groups (Figure 11L).

DISCUSSION

This study investigated the therapeutic effect of EX^{AD}-mito^{Ex} and has brought out several striking preclinical implications. First, we created a reproducible ARDS-SS animal model that closely mimicked the clinical setting of severe ARDS complicated by SS. This model provides crucial sights for clinicians and scientists to test different various therapeutic modalities for ARDS-SS. Second, both *in vitro* and *in vivo* studies proved that mitochondria could be transfused into lung epithelial cells and lung parenchyma potentially providing energy for cell struggling in a harsh environment. Third, both

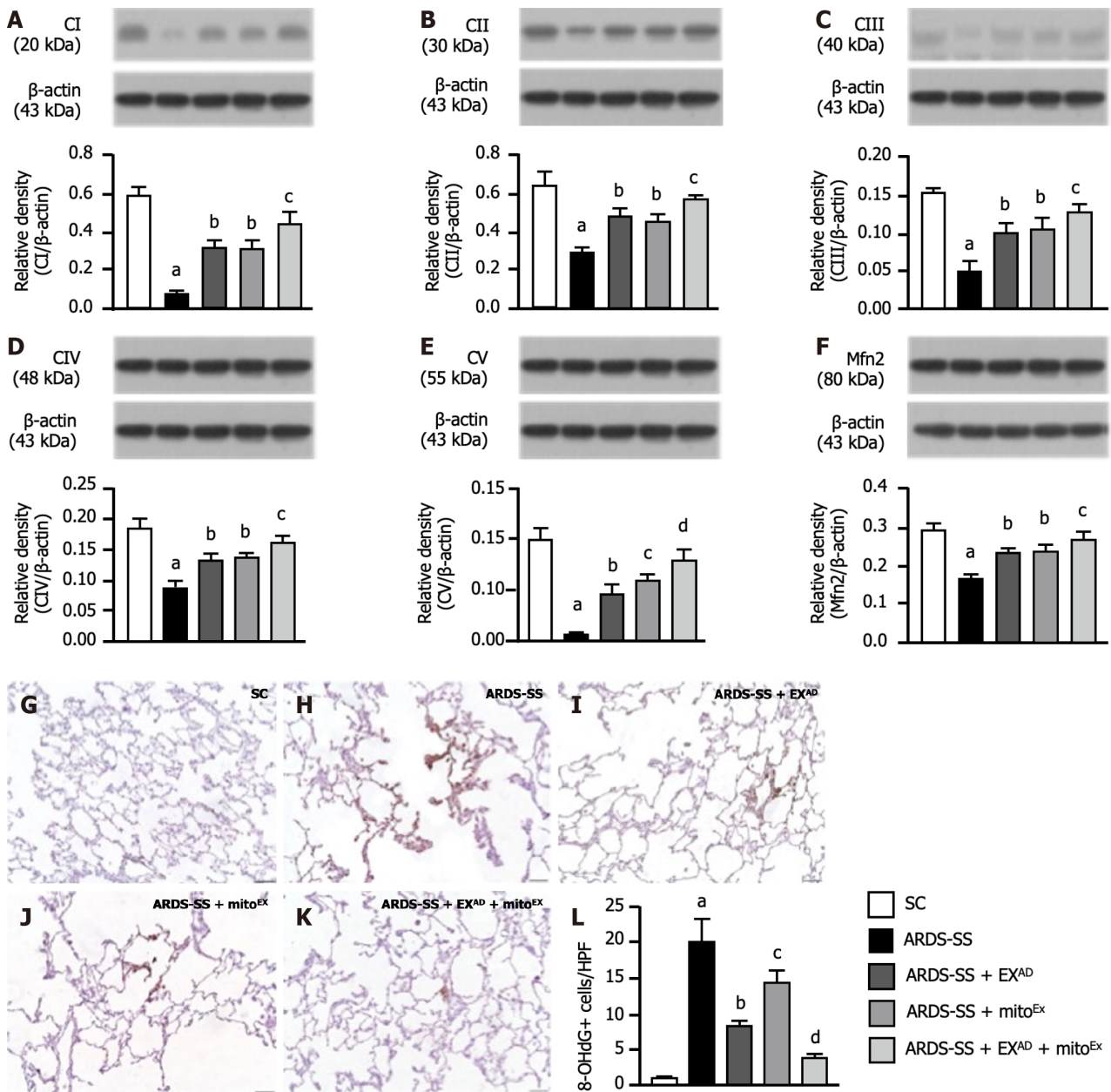


Figure 8 Protein expressions of mitochondrial electron transport chain complexes and mitofusin 2 by day 5 after acute respiratory distress syndrome induction. A: Protein expression of complex I, control vs other groups with different letters, ^a*P* < 0.0001, ^b*P* < 0.001, ^c*P* < 0.01; B: Protein expression of complex II, control vs other groups with different letters, ^a*P* < 0.0001, ^b*P* < 0.001, ^c*P* < 0.01; C: Protein expression of complex III, control vs other groups with different letters, ^a*P* < 0.0001, ^b*P* < 0.001, ^c*P* < 0.01; D: Protein expression of complex IV, control vs other groups with different letters, ^a*P* < 0.0001, ^b*P* < 0.001, ^c*P* < 0.01; E: Protein expression of complex V, control vs other groups with different letters, ^a*P* < 0.0001, ^b*P* < 0.01, ^c*P* < 0.001, ^d*P* < 0.05; F: Protein expression of mitofusin 2, control vs other groups with different letters, ^a*P* < 0.0001, ^b*P* < 0.01, ^c*P* < 0.05; G-K: Illustrating the microscopic finding (400 ×) of immunohistochemical stain for identification of 8-hydroxy-2'-deoxyguanosine (8-OHdG)+ cells (gray color). The scale bars in right lower corner represent 20 μm; L: Analytical result of number of 8-OHdG+ cells, control vs other groups with different letters, ^a*P* < 0.0001, ^b*P* < 0.005, ^c*P* < 0.01, ^d*P* < 0.001. All statistical analyses were performed by one-way ANOVA, followed by Bonferroni multiple comparison post hoc test (*n* = 6 for each group). CI: Complex I; CII: Complex II; CIII: Complex III; CIV: Complex IV; CV: Complex V; Mfn2: Mitofusin 2; 8-OHdG: 8-hydroxy-2'-deoxyguanosine; SC: Sham-operated control; ARDS: Acute respiratory distress syndrome; SS: Sepsis syndrome; mito^{Ex}: Exogenous mitochondria; EX^{AD}: Adipose-derived mesenchymal stem cells-derived exosomes.

in vitro and *in vivo* studies have demonstrated that exosomes had a notable capacity of alleviating inflammation, oxidative stress and apoptosis. Finally, the combined EX^{AD} and mito^{Ex} treatment was better than either treatment alone for protecting lung function and parenchymal integrity against ARDS-SS-induced injury.

Although the etiologies of ARDS-SS have been appraised as multifactorial and the mechanism of ARDS-SS has been extensively discussed to be too complicated to fully understand [1-16], the fundamental damage caused by this disaster is easily realized as the functional unit of the respiratory system, *i.e.*, including the alveoli, ductuli alveola, respiratory bronchioles and capillary networks [9,11,13,21]. The most important finding in the present study was that the lung injury score (*i.e.*, including the reduction in alveolar number and an increase in crowded score) of the functional unit of the respiratory system was remarkably higher increased in ARDS-SS animals than in SC animals. Additionally, SaO₂ (%), an

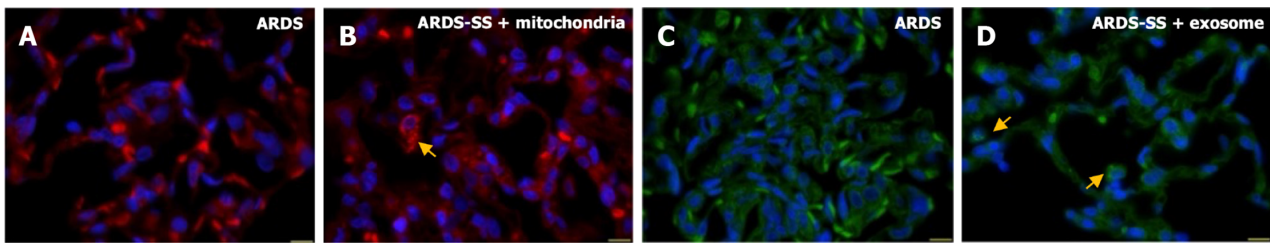


Figure 9 Adipose-derived mesenchymal stem cells-derived exosomes-exogenous mitochondria were identified in the lung parenchyma of acute respiratory distress syndrome rat by day 5 after acute respiratory distress syndrome induction. A and B: Illustrating the immunofluorescent (IF) microscopic finding (1000 ×) of Lipophilic Tracers Dil stain for identification whether the present or absent exogenous mitochondria in acute respiratory distress syndrome (ARDS) group (A) and ARDS-sepsis syndrome (SS) + mitochondria group (B). Noted that no mitochondria were found in ARDS animal. However, numerous mitochondria (red color) (note yellow arrows indicated very small-brilliant particles are mitochondria) were identified in lung parenchyma of ARDS-SS + mitochondria animal; C and D: Illustrating the IF microscopic finding (1000 ×) of Lipophilic Tracers DiO stain for identification whether the present or absent adipose-derived mesenchymal stem cells-derived exosomes in ARDS group (C) and ARDS-SS + exosome group (D). Noted that no exosome was found ARDS animal. However, some exosomes (green color) (note yellow arrows indicate very small particles are exosomes) were identified in lung parenchyma of ARDS-SS + mitochondria animal. The scale bars in right lower corner represent 10 μm. ARDS: Acute respiratory distress syndrome; SS: Sepsis syndrome.

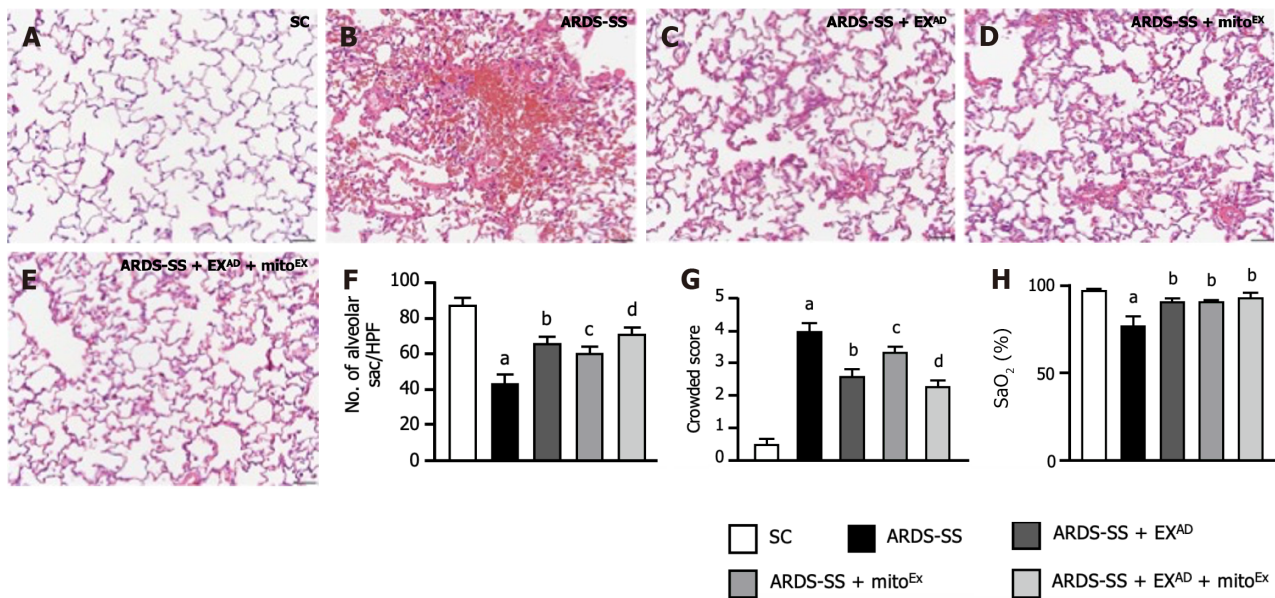


Figure 10 Histopathological findings of lung injury and arterial oxygen saturation by day 5 after acute respiratory distress syndrome induction. A-E: Illustrating the histopathological findings (*i.e.*, hematoxylin and eosin stain) of lung parenchyma by microscope (200 ×) for verifying the lung injury scores (*i.e.*, including variables of alveoli and lung crowding) among the five groups of animals; F: The number of alveolar sacs among five groups. control vs other groups with different letters, ^a*P* < 0.0001, ^b*P* < 0.01, ^c*P* < 0.001, ^d*P* < 0.05; G: Crowded scores of lung parenchyma. control vs other groups with different letters, ^a*P* < 0.0001, ^b*P* < 0.05, ^c*P* < 0.01, ^d*P* < 0.001. The scale bars in right lower corner represent 50 μm; H: Arterial oxygen saturation (SaO₂%), control vs other groups with different letters, ^a*P* < 0.001, ^b*P* < 0.05. All statistical analyses were performed by one-way ANOVA, followed by Bonferroni multiple comparison post hoc test (*n* = 6 for each group). SC: Sham-operated control; ARDS: Acute respiratory distress syndrome; SS: Sepsis syndrome; mito^{EX}: Exogenous mitochondria; EX^{AD}: Adipose-derived mesenchymal stem cells-derived exosomes.

index of lung function capacity, was substantially reduced in the ARDS-SS group compared to that in the SC group. Thus, our findings reinforced those of the previous studies[9,11,13,21]. An important finding of the present study was that combined EX^{AD} and mito^{EX} therapy was notably better than just one therapy in reducing the ARDS-SS-induced lung functional and ultrastructural detriments, highlighting that EX^{AD}-mito^{EX} may be an innovative therapeutic potential for ARDS-SS patients, especially in those patients who are already refractory to conventional therapies.

It is well known that lung fibrosis is a serious complication of ARDS[9,11,13,21,23,24]. An essential finding in the present study was that the lung fibrotic area was substantially upregulated in the ARDS-SS group than in the SC group. Biomarkers, including apoptosis, inflammation, oxidative stress and autophagy which commonly boost the worsening lung fibrosis, were found to be upregulated in the former group compared to the latter group. Our finding, in this way, corroborated with the findings of previous studies[9,11,13,21,23,24]. Interestingly, previous investigations have successfully demonstrated that exosomes therapy effectively preserves lung function and parenchymal integrities against ARDS[25-30]. Another essential finding in the present study was that lung function and architecture were remarkably preserved in ARDS-SS animals with EX^{AD} treatment than without EX^{AD} treatment and further remarkably preserved after combined EX^{AD} and mito^{EX} therapy. Accordingly, our findings, in addition to strengthening the findings of previous

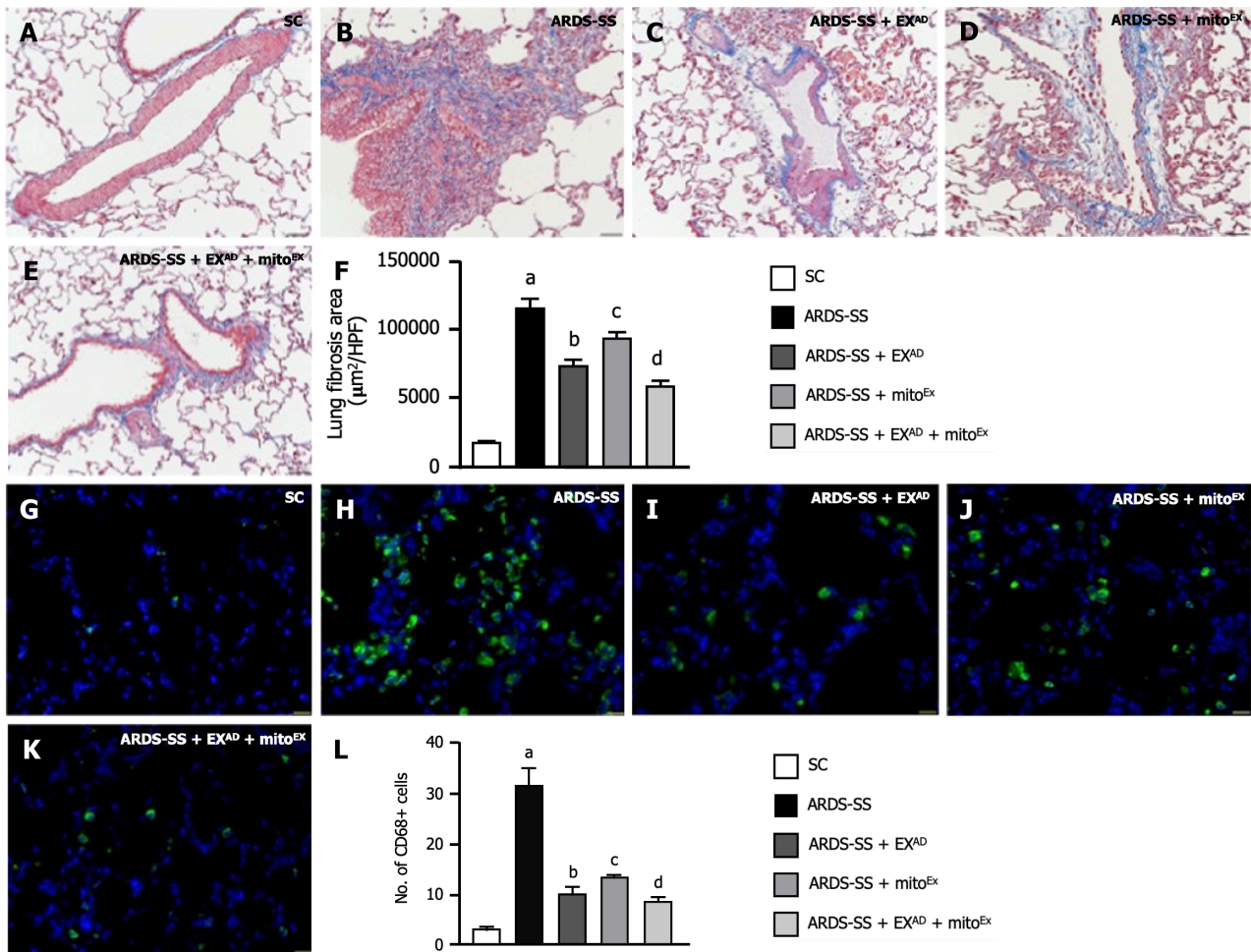


Figure 11 Cellular levels of fibrosis and inflammation by day 5 after acute respiratory distress syndrome induction. A-E: Showing the microscopic finding (200 ×) of Masson’s trichome stain for identification of fibrosis in lung fibrosis (blue color); F: Analytical result of fibrotic area, control vs other groups with different letters, ^a*P* < 0.0001, ^b*P* < 0.05, ^c*P* < 0.01, ^d*P* < 0.001. The scale bars in right lower corner represent 50 µm; G-K: Illustrating the immunofluorescent microscopic finding (400 ×) for identification of cellular expression of CD68 (green color); L: Analytical result of number of CD68+ cells, control vs other groups with different letters, ^a*P* < 0.0001, ^b*P* < 0.05, ^c*P* < 0.01, ^d*P* < 0.001. The scale bars in right lower corner represent 20 µm. All statistical analyses were performed by one-way ANOVA, followed by Bonferroni multiple comparison post hoc test (*n* = 6 for each group). SC: Sham-operated control; ARDS: Acute respiratory distress syndrome; SS: Sepsis syndrome; mito^{Ex}: Exogenous mitochondria; EX^{AD}: Adipose-derived mesenchymal stem cells-derived exosomes.

studies[9,11,13,21,23-30], could, at least in part, explain why the lung injury score and lung fibrosis were significantly attenuated by EX^{AD}-mito^{Ex} therapy.

The underlying mechanism of EX^{AD}-mito^{Ex} therapy which provided impressive and promising effects for improving outcomes in the setting of ARDS-SS draws special attention in the present study; therefore, we feel obligated to explain this issue based on the results of the study. Studies have emphasized that MSC-derived exosomes which contain well-known and unknown components[25] have distinctively inherent features of MSCs, *i.e.*, including anti-inflammation, immunomodulation and tissue regeneration[21,22,30-32]. Additionally, previous studies have shown that not only mito^{Ex} could be transfused into recipient cells[13] but also mitochondria could be transferred from normal donor cells to damaged recipient cells through tunneling nanotube for refreshing the mitochondria-derived ATP/available energy, resulting in the rescue of cells that succumbed to ischemic situation[33]. A principal finding in our *in vitro* study was that exosome therapy protected lung epithelial cells (*i.e.*, L2 cell line) against inflammatory damage. Additionally, another principal finding in the *in vivo* study that compared with the ARDS-SS group, the inflammatory reactions in BAL fluids, both in lung tissue and in systemic circulation, were remarkably suppressed, whereas the cell junction biomarkers were notably preserved in the ARDS-SS group after receiving EX^{AD}-mito^{Ex} therapy. Furthermore, our *in vitro* study also demonstrated that mito^{Ex} could be quite easily transfused into the recipient cells (*i.e.*, L2 cell line), resulting in increased levels of APT, mitDNA and mitochondrial cytochrome C. Moreover, the *in vivo* study demonstrated that the protein expressions of complexes I-V and Mfn2 (*i.e.*, mitochondrial fusion marker) were notably increased in ARDS-SS animals after EX^{AD}-mito^{Ex} therapy. In this way, the results of our *in vitro* and *in vivo* studies not only support the findings of previous studies[21,22,30-33] but also fundamentally explain why EX^{AD}-mito^{Ex} therapy could significantly improve the outcomes in ARDS-SS rats. Collectively, we proposed that the results of this combined therapy offered so called “synergic effect” for those of ARDS-SS rodents cardinaly through rejuvenating cells and refreshing the intracellular mitochondria by mito^{Ex} supply and ensuring the cell survival in ischemic/toxic environment *via* EX^{AD} selfless contribution.

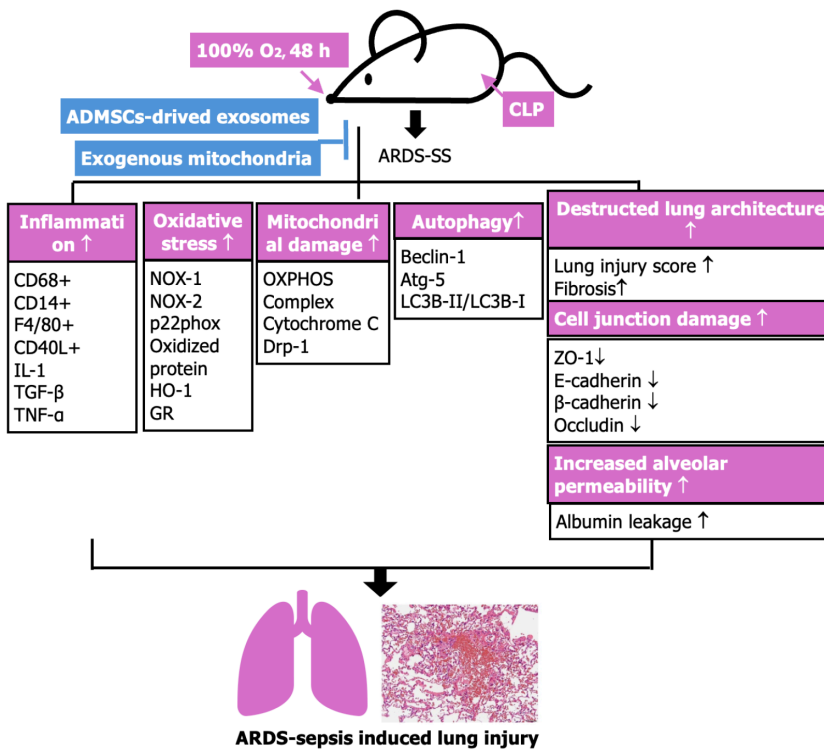


Figure 12 Illustrating the underlying mechanism of combined exogenous mitochondria and adipose-derived mesenchymal stem cell-derived exosomes therapy on protecting the lung parenchyma against acute respiratory distress syndrome-sepsis syndrome induced injury mainly through suppressing inflammation and oxidative stress and refreshing the adenosine triphosphate/mitochondria. ARDS: Acute respiratory distress syndrome; SS: Sepsis syndrome; ADMSC: Adipose-derived mesenchymal stem cell; CLP: Cecal ligation and puncture; IL: Interleukin; TNF: Tumor necrosis factor; TGF: Transforming growth factor; Drp1: Dynamin-related protein 1; Atg5: Autophagy related 5; ZO-1: Zonula occludens-1; HO-1: Heme oxygenase-1; GR: Glutathione reductase; OXPHOS: Oxidative phosphorylation.

The treatment of moderate to severe ARDS remains a formidable challenge, especially in patients with ARDS-SS who are always observed to have extremely high mortality[6-8]. Interestingly, our phase I clinical trial demonstrated that human umbilical cord-derived mesenchymal stem cell therapy could be beneficial for moderate-severe ARDS patients [12]. Based on our previous study[12] and the current results, perhaps, combined EX^{AD}-mito^{Ex} therapy would provide more promising effect for those severe ARDS-SS patients, especially for those who are refractory to conventional therapy.

Study limitation

This study had some limitations. First, although the results are promising, the study period was relatively short. Thus, we do not know whether the long-term outcomes of such a treatment are still promising. Second, it is a common sense that the underlying mechanism of ARDS complicated by SS is definitely more complicated than merely ARDS or SS. Accordingly, we schematically illustrated the proposed underlying mechanism in Figure 12 for elucidating why the EX^{AD}-mito^{Ex} therapy effectively salvaged the lung function and its parenchymal ultrastructural integrity.

CONCLUSION

The results of this study demonstrated that EX^{AD}-mito^{Ex} therapy attenuated the lung parenchymal damage and preserves lung function in rodents with ARDS-SS.

FOOTNOTES

Author contributions: Lin KC and Yeh JN performed the experiments; Fang WF, Chiang JY, Chiang HJ, and Shao PL performed the calculations and aided in interpreting the results; Sung PH and Yip HK conceived this study, drafted and revised the manuscript. Sung PH and Yip HK contributed equally to this work and should be considered co-corresponding authors.

Supported by the Ministry of Science and Technology, Taiwan, No. MOST 110-2314-B-182A-133-.

Institutional animal care and use committee statement: All procedures involving animals were reviewed and approved by the Committee at Kaohsiung Chang Gung Memorial Hospital (Affidavit of Approval of Animal Use Protocol No. 2020121604) and performed in

accordance with the Guide for the Care and Use of Laboratory Animals, 8th edition (NIH publication No. 85-23, National Academy Press, Washington, DC, United States, revised 2011).

Conflict-of-interest statement: All the authors report no relevant conflicts of interest for this article.

Data sharing statement: All data generated or analyzed during this study are included in this published article and its supplementary information files.

ARRIVE guidelines statement: The authors have read the ARRIVE guidelines, and the manuscript was prepared and revised according to the ARRIVE guidelines.

Open-Access: This article is an open-access article that was selected by an in-house editor and fully peer-reviewed by external reviewers. It is distributed in accordance with the Creative Commons Attribution NonCommercial (CC BY-NC 4.0) license, which permits others to distribute, remix, adapt, build upon this work non-commercially, and license their derivative works on different terms, provided the original work is properly cited and the use is non-commercial. See: <https://creativecommons.org/licenses/by-nc/4.0/>

Country of origin: Taiwan

ORCID number: Pei-Hsun Sung 0000-0002-1989-9752; Hon-Kan Yip 0000-0002-6305-5717.

S-Editor: Wang JJ

L-Editor: A

P-Editor: Zhang XD

REFERENCES

- 1 **Gaieski DF**, Edwards JM, Kallan MJ, Carr BG. Benchmarking the incidence and mortality of severe sepsis in the United States. *Crit Care Med* 2013; **41**: 1167-1174 [PMID: 23442987 DOI: 10.1097/CCM.0b013e31827c09f8]
- 2 **Hudson LD**, Steinberg KP. Epidemiology of acute lung injury and ARDS. *Chest* 1999; **116**: 74S-82S [PMID: 10424602 DOI: 10.1378/chest.116.suppl_1.74S-a]
- 3 **Rubinfeld GD**, Caldwell E, Peabody E, Weaver J, Martin DP, Neff M, Stern EJ, Hudson LD. Incidence and outcomes of acute lung injury. *N Engl J Med* 2005; **353**: 1685-1693 [PMID: 16236739 DOI: 10.1056/NEJMoa050333]
- 4 **Stapleton RD**, Wang BM, Hudson LD, Rubinfeld GD, Caldwell ES, Steinberg KP. Causes and timing of death in patients with ARDS. *Chest* 2005; **128**: 525-532 [PMID: 16100134 DOI: 10.1378/chest.128.2.525]
- 5 **Acute Respiratory Distress Syndrome Network**, Brower RG, Matthay MA, Morris A, Schoenfeld D, Thompson BT, Wheeler A. Ventilation with lower tidal volumes as compared with traditional tidal volumes for acute lung injury and the acute respiratory distress syndrome. *N Engl J Med* 2000; **342**: 1301-1308 [PMID: 10793162 DOI: 10.1056/NEJM200005043421801]
- 6 **National Heart, Lung, and Blood Institute PETAL Clinical Trials Network**, Moss M, Huang DT, Brower RG, Ferguson ND, Ginde AA, Gong MN, Grissom CK, Gundle S, Hayden D, Hite RD, Hou PC, Hough CL, Iwashyna TJ, Khan A, Liu KD, Talmor D, Thompson BT, Ulysse CA, Yealy DM, Angus DC. Early Neuromuscular Blockade in the Acute Respiratory Distress Syndrome. *N Engl J Med* 2019; **380**: 1997-2008 [PMID: 31112383 DOI: 10.1056/NEJMoa1901686]
- 7 **Levitt JE**, Matthay MA. Clinical review: Early treatment of acute lung injury--paradigm shift toward prevention and treatment prior to respiratory failure. *Crit Care* 2012; **16**: 223 [PMID: 22713281 DOI: 10.1186/cc11144]
- 8 **Combes A**, Hajage D, Capellier G, Demoule A, Lavoué S, Guervilly C, Da Silva D, Zafrani L, Tirot P, Veber B, Maury E, Levy B, Cohen Y, Richard C, Kalfon P, Bouadma L, Mehdaoui H, Beduneau G, Lebreton G, Brochard L, Ferguson ND, Fan E, Slutsky AS, Brodie D, Mercat A; EOLIA Trial Group, REVA, and ECMONet. Extracorporeal Membrane Oxygenation for Severe Acute Respiratory Distress Syndrome. *N Engl J Med* 2018; **378**: 1965-1975 [PMID: 29791822 DOI: 10.1056/NEJMoa1800385]
- 9 **Sun CK**, Lee FY, Kao YH, Chiang HJ, Sung PH, Tsai TH, Lin YC, Leu S, Wu YC, Lu HI, Chen YL, Chung SY, Su HL, Yip HK. Systemic combined melatonin-mitochondria treatment improves acute respiratory distress syndrome in the rat. *J Pineal Res* 2015; **58**: 137-150 [PMID: 25491480 DOI: 10.1111/jpi.12199]
- 10 **Day YJ**, Chen KH, Chen YL, Huang TH, Sung PH, Lee FY, Chen CH, Chai HT, Yin TC, Chiang HJ, Chung SY, Chang HW, Yip HK. Preactivated and Disaggregated Shape-Changed Platelets Protected Against Acute Respiratory Distress Syndrome Complicated by Sepsis Through Inflammation Suppression. *Shock* 2016; **46**: 575-586 [PMID: 27058048 DOI: 10.1097/SHK.0000000000000617]
- 11 **Chen CH**, Chen YL, Sung PH, Sun CK, Chen KH, Huang TH, Lu HI, Lee FY, Sheu JJ, Chung SY, Lee MS, Yip HK. Effective protection against acute respiratory distress syndrome/sepsis injury by combined adipose-derived mesenchymal stem cells and preactivated disaggregated platelets. *Oncotarget* 2017; **8**: 82415-82429 [PMID: 29137274 DOI: 10.18632/oncotarget.19312]
- 12 **Yip HK**, Fang WF, Li YC, Lee FY, Lee CH, Pei SN, Ma MC, Chen KH, Sung PH, Lee MS. Human Umbilical Cord-Derived Mesenchymal Stem Cells for Acute Respiratory Distress Syndrome. *Crit Care Med* 2020; **48**: e391-e399 [PMID: 32187077 DOI: 10.1097/CCM.0000000000004285]
- 13 **Lin KC**, Wallace CG, Yin TC, Sung PH, Chen KH, Lu HI, Chai HT, Chen CH, Chen YL, Li YC, Shao PL, Lee MS, Sheu JJ, Yip HK. Shock Wave Therapy Enhances Mitochondrial Delivery into Target Cells and Protects against Acute Respiratory Distress Syndrome. *Mediators Inflamm* 2018; **2018**: 5425346 [PMID: 30420790 DOI: 10.1155/2018/5425346]
- 14 **Matthay MA**, Ware LB, Zimmerman GA. The acute respiratory distress syndrome. *J Clin Invest* 2012; **122**: 2731-2740 [PMID: 22850883 DOI: 10.1172/JCI60331]
- 15 **Vandenbroucke E**, Mehta D, Minshall R, Malik AB. Regulation of endothelial junctional permeability. *Ann N Y Acad Sci* 2008; **1123**: 134-

- 145 [PMID: [18375586](#) DOI: [10.1196/annals.1420.016](#)]
- 16 **Bachofen M**, Weibel ER. Alterations of the gas exchange apparatus in adult respiratory insufficiency associated with septicemia. *Am Rev Respir Dis* 1977; **116**: 589-615 [PMID: [921049](#) DOI: [10.1164/arrd.1977.116.4.589](#)]
- 17 **Yip HK**, Shao PL, Wallace CG, Sheu JJ, Sung PH, Lee MS. Early intramyocardial implantation of exogenous mitochondria effectively preserved left ventricular function in doxorubicin-induced dilated cardiomyopathy rat. *Am J Transl Res* 2020; **12**: 4612-4627 [PMID: [32913535](#)]
- 18 **Chen HH**, Chen YT, Yang CC, Chen KH, Sung PH, Chiang HJ, Chen CH, Chua S, Chung SY, Chen YL, Huang TH, Kao GS, Chen SY, Lee MS, Yip HK. Melatonin pretreatment enhances the therapeutic effects of exogenous mitochondria against hepatic ischemia-reperfusion injury in rats through suppression of mitochondrial permeability transition. *J Pineal Res* 2016; **61**: 52-68 [PMID: [26993080](#) DOI: [10.1111/jpi.12326](#)]
- 19 **Ko SF**, Chen YL, Sung PH, Chiang JY, Chu YC, Huang CC, Huang CR, Yip HK. Hepatic (31) P-magnetic resonance spectroscopy identified the impact of melatonin-pretreated mitochondria in acute liver ischaemia-reperfusion injury. *J Cell Mol Med* 2020; **24**: 10088-10099 [PMID: [32691975](#) DOI: [10.1111/jcmm.15617](#)]
- 20 **Huang TH**, Chung SY, Chua S, Chai HT, Sheu JJ, Chen YL, Chen CH, Chang HW, Tong MS, Sung PH, Sun CK, Lu HI, Yip HK. Effect of early administration of lower dose versus high dose of fresh mitochondria on reducing monocrotaline-induced pulmonary artery hypertension in rat. *Am J Transl Res* 2016; **8**: 5151-5168 [PMID: [28077992](#)]
- 21 **Sun CK**, Chen CH, Chang CL, Chiang HJ, Sung PH, Chen KH, Chen YL, Chen SY, Kao GS, Chang HW, Lee MS, Yip HK. Melatonin treatment enhances therapeutic effects of exosomes against acute liver ischemia-reperfusion injury. *Am J Transl Res* 2017; **9**: 1543-1560 [PMID: [28469765](#)]
- 22 **Ko SF**, Yip HK, Zhen YY, Lee CC, Huang CC, Ng SH, Lin JW. Adipose-Derived Mesenchymal Stem Cell Exosomes Suppress Hepatocellular Carcinoma Growth in a Rat Model: Apparent Diffusion Coefficient, Natural Killer T-Cell Responses, and Histopathological Features. *Stem Cells Int* 2015; **2015**: 853506 [PMID: [26345219](#) DOI: [10.1155/2015/853506](#)]
- 23 **Wendisch D**, Dietrich O, Mari T, von Stillfried S, Ibarra IL, Mittermaier M, Mache C, Chua RL, Knoll R, Timm S, Brumhard S, Krammer T, Zauber H, Hiller AL, Pascual-Reguant A, Mothes R, Bülow RD, Schulze J, Leopold AM, Djudjaj S, Erhard F, Geffers R, Pott F, Kazmierski J, Radke J, Pergantis P, Baßler K, Conrad C, Aschenbrenner AC, Sawitzki B, Landthaler M, Wyler E, Horst D; Deutsche COVID-19 OMICS Initiative (DeCOI), Hippenstiel S, Hocke A, Heppner FL, Uhrig A, Garcia C, Machleidt F, Herold S, Elez Kurtaj S, Thibeault C, Witzernath M, Cochain C, Suttorp N, Drosten C, Goffinet C, Kurth F, Schultze JL, Radbruch H, Ochs M, Eils R, Müller-Redetzky H, Hauser AE, Luecken MD, Theis FJ, Conrad C, Wolff T, Boor P, Selbach M, Saliba AE, Sander LE. SARS-CoV-2 infection triggers profibrotic macrophage responses and lung fibrosis. *Cell* 2021; **184**: 6243-6261.e27 [PMID: [34914922](#) DOI: [10.1016/j.cell.2021.11.033](#)]
- 24 **Michalski JE**, Kurche JS, Schwartz DA. From ARDS to pulmonary fibrosis: the next phase of the COVID-19 pandemic? *Transl Res* 2022; **241**: 13-24 [PMID: [34547499](#) DOI: [10.1016/j.trsl.2021.09.001](#)]
- 25 **Willis GR**, Fernandez-Gonzalez A, Anastas J, Vitali SH, Liu X, Ericsson M, Kwong A, Mitsialis SA, Kourembanas S. Mesenchymal Stromal Cell Exosomes Ameliorate Experimental Bronchopulmonary Dysplasia and Restore Lung Function through Macrophage Immunomodulation. *Am J Respir Crit Care Med* 2018; **197**: 104-116 [PMID: [28853608](#) DOI: [10.1164/rccm.201705-0925OC](#)]
- 26 **Deng H**, Wu L, Liu M, Zhu L, Chen Y, Zhou H, Shi X, Wei J, Zheng L, Hu X, Wang M, He Z, Lv X, Yang H. Bone Marrow Mesenchymal Stem Cell-Derived Exosomes Attenuate LPS-Induced ARDS by Modulating Macrophage Polarization Through Inhibiting Glycolysis in Macrophages. *Shock* 2020; **54**: 828-843 [PMID: [32433208](#) DOI: [10.1097/SHK.0000000000001549](#)]
- 27 **Dinh PC**, Paudel D, Brochu H, Popowski KD, Gracieux MC, Cores J, Huang K, Hensley MT, Harrell E, Vandergriff AC, George AK, Barrio RT, Hu S, Allen TA, Blackburn K, Caranasos TG, Peng X, Schnabel LV, Adler KB, Lobo LJ, Goshe MB, Cheng K. Inhalation of lung spheroid cell secretome and exosomes promotes lung repair in pulmonary fibrosis. *Nat Commun* 2020; **11**: 1064 [PMID: [32111836](#) DOI: [10.1038/s41467-020-14344-7](#)]
- 28 **Kaspi H**, Semo J, Abramov N, Dekel C, Lindborg S, Kern R, Lebovits C, Aricha R. MSC-NTF (NurOwn®) exosomes: a novel therapeutic modality in the mouse LPS-induced ARDS model. *Stem Cell Res Ther* 2021; **12**: 72 [PMID: [33468250](#) DOI: [10.1186/s13287-021-02143-w](#)]
- 29 **Liu X**, Gao C, Wang Y, Niu L, Jiang S, Pan S. BMSC-Derived Exosomes Ameliorate LPS-Induced Acute Lung Injury by miR-384-5p-Controlled Alveolar Macrophage Autophagy. *Oxid Med Cell Longev* 2021; **2021**: 9973457 [PMID: [34234888](#) DOI: [10.1155/2021/9973457](#)]
- 30 **Liu C**, Xiao K, Xie L. Advances in the use of exosomes for the treatment of ALI/ARDS. *Front Immunol* 2022; **13**: 971189 [PMID: [36016948](#) DOI: [10.3389/fimmu.2022.971189](#)]
- 31 **Chang CL**, Chen HH, Chen KH, Chiang JY, Li YC, Lin HS, Sung PH, Yip HK. Adipose-derived mesenchymal stem cell-derived exosomes markedly protected the brain against sepsis syndrome induced injury in rat. *Am J Transl Res* 2019; **11**: 3955-3971 [PMID: [31396312](#)]
- 32 **Chang CL**, Chen CH, Chiang JY, Sun CK, Chen YL, Chen KH, Sung PH, Huang TH, Li YC, Chen HH, Yip HK. Synergistic effect of combined melatonin and adipose-derived mesenchymal stem cell (ADMSC)-derived exosomes on amelioration of dextran sulfate sodium (DSS)-induced acute colitis. *Am J Transl Res* 2019; **11**: 2706-2724 [PMID: [31217848](#)]
- 33 **Yip HK**, Dubey NK, Lin KC, Sung PH, Chiang JY, Chu YC, Huang CR, Chen YL, Deng YH, Cheng HC, Deng WP. Melatonin rescues cerebral ischemic events through upregulated tunneling nanotube-mediated mitochondrial transfer and downregulated mitochondrial oxidative stress in rat brain. *Biomed Pharmacother* 2021; **139**: 111593 [PMID: [33865018](#) DOI: [10.1016/j.biopha.2021.111593](#)]



Published by **Baishideng Publishing Group Inc**
7041 Koll Center Parkway, Suite 160, Pleasanton, CA 94566, USA
Telephone: +1-925-3991568
E-mail: office@baishideng.com
Help Desk: <https://www.f6publishing.com/helpdesk>
<https://www.wjgnet.com>

